



Night-time measurements of HO_x during the RONOCO project and analysis of the sources of HO₂

H. M. Walker¹, D. Stone¹, T. Ingham^{1,2}, S. Vaughan¹, M. Cain^{3,4}, R. L. Jones³, O. J. Kennedy³, M. McLeod³, B. Ouyang³, J. Pyle^{3,4}, S. Bauguitte^{5,6}, B. Bandy^{7,8}, G. Forster^{7,8}, M. J. Evans^{9,10}, J. F. Hamilton⁹, J. R. Hopkins^{9,10}, J. D. Lee^{9,10}, A. C. Lewis^{9,10}, R. T. Lidster⁹, S. Punjabi^{9,10}, W. T. Morgan^{11,12}, and D. E. Heard^{1,2}

¹School of Chemistry, University of Leeds, Leeds, UK

²National Centre for Atmospheric Science, University of Leeds, Leeds, UK

³Department of Chemistry, University of Cambridge, Cambridge, UK

⁴National Centre for Atmospheric Science, University of Cambridge, Cambridge, UK

⁵Facility for Airborne Atmospheric Measurements (FAAM), Cranfield University, Cranfield, UK

⁶National Centre for Atmospheric Science, FAAM, Cranfield University, Cranfield, UK

⁷Centre for Ocean and Atmospheric Sciences, School of Environmental Sciences, University of East Anglia, Norwich, UK

⁸National Centre for Atmospheric Science, University of East Anglia, Norwich, UK

⁹Wolfson Atmospheric Chemistry Laboratories, Department of Chemistry, University of York, York, UK

¹⁰National Centre for Atmospheric Science, University of York, York, UK

¹¹School of Earth, Atmospheric and Environmental Sciences, University of Manchester, Manchester, UK

¹²National Centre for Atmospheric Science, University of Manchester, Manchester, UK

Correspondence to: D. E. Heard (d.e.heard@leeds.ac.uk)

Received: 6 November 2014 – Published in Atmos. Chem. Phys. Discuss.: 30 January 2015

Revised: 12 May 2015 – Accepted: 24 May 2015 – Published: 23 July 2015

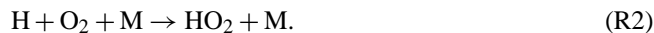
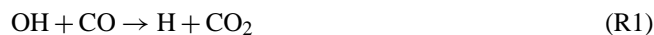
Abstract. Measurements of the radical species OH and HO₂ were made using the fluorescence assay by gas expansion (FAGE) technique during a series of night-time and daytime flights over the UK in summer 2010 and winter 2011. OH was not detected above the instrument's 1σ limit of detection during any of the night-time flights or during the winter daytime flights, placing upper limits on [OH] of 1.8×10^6 molecule cm⁻³ and 6.4×10^5 molecule cm⁻³ for the summer and winter flights, respectively. HO₂ reached a maximum concentration of 3.2×10^8 molecule cm⁻³ (13.6 pptv) during a night-time flight on 20 July 2010, when the highest concentrations of NO₃ and O₃ were also recorded. An analysis of the rates of reaction of OH, O₃, and the NO₃ radical with measured alkenes indicates that the summer night-time troposphere can be as important for the processing of volatile organic compounds (VOCs) as the winter daytime troposphere. An analysis of the instantaneous rate of production of HO₂ from the reactions of O₃ and NO₃ with alkenes has shown that, on

average, reactions of NO₃ dominated the night-time production of HO₂ during summer and reactions of O₃ dominated the night-time HO₂ production during winter.

1 Introduction

Trace gases emitted into the atmosphere, including pollutants and greenhouse gases, are removed primarily by oxidation. The hydroxyl radical, OH, is the most important oxidising species in the daytime troposphere, reacting with numerous species, including volatile organic compounds (VOCs), CO, SO₂, and long-lived anthropogenic halogenated compounds. During the day, primary production of OH (i.e. initialisation of the radical chain) occurs predominantly via photolysis of ozone at $\lambda \leq 340$ nm, followed by the reaction of the resulting electronically excited oxygen atom, O(¹D), with water vapour. The OH-initiated oxidation of VOCs leads to the production of the hydroperoxy radical, HO₂, and together the

two radicals form the HO_x family. A key reaction in the conversion of OH to HO₂ is the reaction with CO:



The reaction of OH with VOCs results in the production of organic peroxy radicals, RO₂:



Reactions of HO₂ and RO₂ with NO propagate the HO_x radical chain, regenerating OH:



The production of OH through the photolysis of ozone (and other species at longer wavelengths) is limited to daylight hours, and the oxidation of trace gases at night proceeds through alternative mechanisms. Two mechanisms are known to initiate HO_x radical chemistry and oxidation chemistry at night: ozonolysis of alkenes and reactions of the nitrate radical, NO₃, with alkenes.

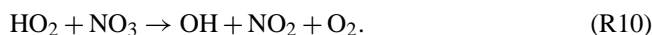
Reactions of ozone with alkenes occur via the addition of ozone to the double bond to form a five-membered ring called a primary ozonide. The primary ozonide decomposes to form one of two possible pairs of products, each pair consisting of a carbonyl compound and a vibrationally and rotationally excited carbonyl oxide termed a Criegee intermediate (CI). The simplest gas-phase CI, CH₂OO, and the alkyl-substituted CH₃CHOO have been observed directly by photoionisation mass spectrometry (Taatjes et al., 2008, 2012, 2013; Beames et al., 2012, 2013; Welz et al., 2012; Stone et al., 2014a), by infrared absorption spectroscopy (Su et al., 2013), and by microwave spectroscopy (Nakajima and Endo, 2013, 2014). Excited CIs may be stabilised by collision with surrounding molecules (Donahue et al., 2011; Drozd and Donahue, 2011) or may undergo isomerisation or decomposition to yield products including OH, H, and subsequently HO₂ (Paulson and Orlando, 1996; Kroll et al., 2001a, b, 2002; Johnson and Marston, 2008). Stabilised CIs (SCIs) are known to react with a variety of compounds, including H₂O, NO₂, SO₂, and a variety of organic compounds (e.g. Mauldin III et al., 2012; Taatjes et al., 2012, 2013, 2014; Ouyang et al., 2013; Stone et al., 2014a). There is experimental evidence for the formation of OH from the thermal decomposition of SCIs, on a much longer timescale than the decomposition or isomerisation of excited CIs (Kroll et al., 2001a, b). The OH produced through these ozonolysis mechanisms will proceed to oxidise other VOC species. Criegee intermediates formed in the ozonolysis of alkenes are known to be an important source of HO_x during the day and at night (Paulson and Orlando, 1996; Donahue et al., 1998; Kanaya et al., 1999; Salisbury et al., 2001; Geyer et al., 2003; Ren et al., 2003a, 2006;

Heard et al., 2004; Harrison et al., 2006; Sommariva et al., 2007). The gas-phase ozonolysis of unsaturated VOCs, and in particular the role and subsequent chemistry of the Criegee intermediate, have been reviewed in detail by Johnson and Marston (2008), Donahue et al. (2011), Vereecken and Francisco (2012), and Taatjes et al. (2014).

Another key night-time oxidant, NO₃, is formed primarily by the reaction of NO₂ with ozone. NO₃ reacts with a range of species in the troposphere, and its reaction with alkenes is known to be an important night-time oxidation mechanism (Salisbury et al., 2001; Geyer et al., 2003; Sommariva et al., 2007; Emmerson and Carslaw, 2009; Brown et al., 2011). The reaction between NO₃ and an alkene proceeds primarily via addition to a double bond to form a nitrooxyalkyl radical, R-ONO₂. At atmospheric pressure, the main fate of the nitrooxyalkyl radical is reaction with O₂ (Berndt and Böge, 1994) to produce a nitrooxyalkyl peroxy radical, O₂-R-ONO₂. The nitrooxyalkyl peroxy radical can react with NO₂, HO₂, RO₂, NO, and NO₃, of which the latter two reactions lead to the formation of the nitrooxyalkoxy radical, O-R-ONO₂. The nitrooxyalkoxy radical can undergo isomerisation, decomposition, or reaction with O₂. Reaction with O₂, analogous to the reaction of organic alkoxy radicals, yields HO₂:



Thus, the night-time oxidation of hydrocarbons by NO₃ leads to the production of HO₂. The reaction of HO₂ with NO (Reaction R7), O₃, and NO₃ can generate OH:



Atkinson and Arey (2003) published a detailed review of the tropospheric degradation of VOCs, including reaction with O₃ and NO₃. A comprehensive review of night-time radical chemistry is given by Brown and Stutz (2012).

The oxidising capacity of the nocturnal troposphere is thought to be controlled by the reactions described above, with a limited role for OH and HO₂ due to the absence of their photolytic sources. The oxidation of VOCs at night can have significant effects on daytime air quality and tropospheric ozone production (Brown et al., 2004, 2006, 2011; Wong and Stutz, 2010). Several field measurement campaigns have involved night-time measurements of OH, HO₂, RO₂, and NO₃ (see Table 1) and have highlighted the importance of the vertical profile of night-time radical concentrations and chemistry (Geyer and Stutz, 2004a, b; Stutz et al., 2004; Volkamer et al., 2010), but prior to the current work, there had been no aircraft-based studies of night-time chemistry involving measurements of both NO₃ and HO₂ to enable the vertical profiling of the lower atmosphere and a full evaluation of the nocturnal radical budget. Table 1 gives details of some previous measurements and modelling of night-time

Table 1. Examples of modelling studies and observations of HO_x radicals and VOC oxidation at night. PERCA: peroxy radical chemical amplification; LIF: laser-induced fluorescence; DOAS: differential optical absorption spectroscopy; MCM: Master Chemical Mechanism; MIESR: matrix isolation electron spin resonance; RACM: Regional Atmospheric Chemistry Mechanism; CRDS: cavity ring-down spectroscopy; CIMS: chemical ionisation mass spectrometry; GC: gas chromatography; PTRMS: proton transfer reaction mass spectrometry; FTIR: Fourier transform infrared spectroscopy; DUALER: DUAL channel peroxy radical chemical amplifier; OA-CRD: off-axis cavity ring-down spectroscopy; CRM-PTR-MS: comparative reactivity method proton transfer mass spectrometry.

Location, campaign, date	Methods	Results	Reference
Mace Head, Ireland, Eastern Atlantic Spring Experiment (EASE97), 1997	Measurements: [HO ₂ +RO ₂] measured by PERCA; HO _x measured by LIF; NO ₃ measured by DOAS. Modelling: campaign-tailored box model constrained to measurements, based on MCM.	Two nights of HO _x measurements: HO ₂ = 1–2 and 0.5–0.7 pptv; OH not detected above limit of detection (~2.5 × 10 ⁵ cm ⁻³). NO ₃ dominated radical production in westerly (clean) air masses; O ₃ dominated in NE, SE, and SW air masses and dominated radical production overall during the campaign.	Salisbury et al. (2001); Creasey et al. (2002)
Pabstthum, Germany, Berlin Ozone Experiment (BERLIOZ), 1998	Measurements: HO _x measured by LIF; NO ₃ measured by DOAS and MIESR. Modelling: zero-dimensional model using lumped VOC reactivity, constrained to measured species.	Night-time OH = 1.85 × 10 ⁵ cm ⁻³ , compared to modelled value of 4.1 × 10 ⁵ cm ⁻³ . Night-time HO ₂ = 3 × 10 ⁷ cm ⁻³ , model results in agreement. NO ₃ chemistry responsible for 53 % of HO ₂ and 36 % of OH during the night. O ₃ + alkene responsible for 47 % of HO ₂ and 64 % of OH during the night.	Geyer et al. (2003); Holland et al. (2003)
Birmingham, Pollution of the Urban Midlands Atmosphere (PUMA), 1999 and 2000	Measurements: HO _x measured by LIF. Modelling: photochemical box model constrained to measurements, based on MCM.	Daytime OH initiation dominated by O ₃ + alkenes, HONO photolysis, and O(¹ D) + H ₂ O during summer. O ₃ + alkenes dominated in winter. O ₃ + alkenes main radical source at night.	Emmerson et al. (2005); Harrison et al. (2006)
New York, PM _{2.5} Technology Assessment and Characteristics Study-New York (PMTACS-NY), 2001	Measurements: HO _x measured by LIF.	Night-time OH ~ 7 × 10 ⁵ cm ⁻³ and night-time HO ₂ ~ 8 × 10 ⁶ cm ⁻³ . Increase in HO _x after midnight attributed to increase in O ₃ due to transport. O ₃ + alkenes main source of night-time HO _x .	Ren et al. (2003a, b)
Mace Head, North Atlantic Marine Boundary Layer Experiment (NAMBLEX), 2002	Measurements: HO _x measured by LIF; NO ₃ measured by DOAS. Modelling: zero-dimensional box models constrained to measured species, based on MCM.	Night-time HO ₂ = 2–3 × 10 ⁷ cm ⁻³ ; OH below detection limit (6 × 10 ⁴ cm ⁻³). Model overestimated HO ₂ . On average, O ₃ + alkene reactions contributed 59 % and NO ₃ + alkene reactions contributed 41 % to RO ₂ production at night, but NO ₃ and RO ₂ concentrations were always higher in semi-polluted air masses than in clean marine air masses and NO ₃ reactions dominated in these conditions.	Fleming et al. (2006); Smith et al. (2006); Sommariva et al. (2007)
Writtle, London, Tropospheric ORganic CHemistry experiment (TORCH), 2003	Measurements: HO _x measured by LIF, RO ₂ measured by PERCA, during a heatwave or pollution episode. Modelling: zero-dimensional box model constrained to measured species.	OH and HO ₂ observed above the limit of detection on several nights. OH peaked at 8.5 × 10 ⁵ cm ⁻³ ; HO ₂ peaked at 1 × 10 ⁸ cm ⁻³ . Model overpredicted night-time OH and HO ₂ on average by 24 % and 7 % and underpredicted [HO ₂ + ΣRO ₂] by 22 %.	Lee et al. (2006); Emmerson et al. (2007); Emmerson and Carslaw (2009)
Mexico City Metropolitan Area (MCMA 2003)	Measurements: HO _x measured by LIF, NO ₃ measured by DOAS. Modelling: zero-dimensional model based on MCM v3.1, constrained to measured species.	Polluted city location characterised by high levels of NO, NO ₂ , and O ₃ . Maximum night-time OH ~ 1 × 10 ⁶ cm ⁻³ ; maximum night-time HO ₂ ~ 6 pptv. Night-time production of radicals dominated by O ₃ + alkene reactions (76–92 %); NO ₃ + alkene plays a minor role. Daytime radical production ~ 25 times higher than night.	Shirley et al. (2006); Sheehy et al. (2010); Volkamer et al. (2010)
New York City, PMTACS-NY winter 2004	Measurements: HO _x measured by LIF. Modelling: zero-dimensional model based on RACM and constrained by measurements.	Mean maximum OH = 0.05 pptv; mean maximum HO ₂ = 0.7 pptv. Model underprediction of HO ₂ was pronounced when NO was high. O ₃ + alkene reactions were dominant night-time source.	Ren et al. (2006)

Table 1. Continued.

Gulf of Maine, Northeast United States, New England Air Quality Study (NEAQS), 2004	Measurements: NO ₃ and N ₂ O ₅ measured by CRDS. Modelling: zero-dimensional model based on MCM v3.1, constrained to measured species. No measurements of OH, HO ₂ , or RO ₂ .	Ship-based measurements onboard <i>RV Ronald H. Brown</i> in the Gulf of Maine, influenced by unpolluted marine air masses and polluted air masses from the USA and Canada. Maximum modelled night-time HO ₂ = 7.0 × 10 ⁸ cm ⁻³ . Base model overestimated NO ₃ and NO ₂ observations by 30–50%. In anthropogenic air masses, reaction with VOCs and RO ₂ each accounted for 40% of modelled NO ₃ loss.	Sommariva et al. (2009)
Houston, Texas, Texas Air Quality Study (Tex-AQS), 2006	Measurements: NO ₃ and N ₂ O ₅ measured by CRDS; VOCs measured by CIMS, GC, and PTRMS. No direct measurements of OH, HO ₂ , or RO ₂ .	Loss rates and budgets of NO ₃ and highly reactive VOCs calculated. NO ₃ primarily lost through reaction with VOCs. VOC oxidation dominated by NO ₃ , which was 3–5 times more important than O ₃ .	Brown et al. (2011)
Pearl River Delta, China, Program of Regional Integrated Experiments of Pearl River Delta Region (PRIDE-PRD), 2006	Measurements: HO _x measured by LIF; OH reactivity measured by laser-flash photolysis and LIF; VOCs measured by FTIR and GC. Modelling: box model based on RACM and the Mainz Isoprene Mechanism and constrained by measurements.	Rural site 60 km downwind of large urban region (Guangzhou), with low local wind speeds favouring accumulation of air pollutants. Maximum night-time OH (hourly average) = 5 × 10 ⁶ cm ⁻³ ; maximum night-time HO ₂ (hourly average) = 1 × 10 ⁹ cm ⁻³ . Unknown recycling mechanism required for the model to reproduce measured night-time values. OH reactivity peaked at night. Missing night-time reactivity attributed to unmeasured secondary organic compounds.	Lou et al. (2010); Lu et al. (2012, 2013)
Beijing, Campaigns of Air Quality Research in Beijing and Surrounding Regions (CAREBEIJING2006), 2006	Measurements: HO _x measured by LIF; OH lifetime measured by laser-flash photolysis and LIF; VOCs measured by GC. Modelling: box model based on RACM and the Mainz Isoprene Mechanism and constrained by measurements.	Suburban rural site south of Beijing, under the influence of slowly moving, aged polluted air from the south. OH reactivity peaked at night. Model generally underestimated observed night-time OH concentrations.	Lu et al. (2013, 2014)
Cape Verde, Reactive Halogens in the Marine Boundary Layer (RHAMBLe), 2007	Measurements: HO _x measured by LIF. Modelling: box model based on MCM with added halogen chemistry scheme, constrained to measurements of long-lived species.	Clean tropical Atlantic measurement site with occasional continental influence. OH was not measured at night. HO ₂ was detected on two nights, up to 2.5 × 10 ⁷ cm ⁻³ . Model underprediction of HO ₂ was significantly reduced by constraining the model to 100 pptv of peroxy acetyl nitrate (PAN) at night.	Whalley et al. (2010)
Huelva, Spain, Diel Oxidant Mechanisms in relation to Nitrogen Oxides (DOMINO), 2008	Measurements: [HO ₂ +RO ₂] measured by DUALER; HO _x measured by LIF; NO ₃ and N ₂ O ₅ measured by OA-CRD; OH reactivity measured by CRM-PTR-MS. No measurements of anthropogenic VOCs.	Coastal forested site with strong urban-industrial and weak biogenic influences. Maxima in [HO ₂ +RO ₂] and [HO ₂] were observed around noon and midnight. Enhanced night-time [HO ₂ +RO ₂] (up to 80 pptv) was observed in air masses from the urban-industrial region. Maximum night-time HO ₂ = 8 pptv. Measured NO ₃ was generally below LOD; calculated NO ₃ up to 20 pptv. Calculated production of RO ₂ from NO ₃ + alkenes accounts for 47–54% of observed [HO ₂ +RO ₂]. Ozonolysis of unmeasured alkenes could account for remaining [HO ₂ +RO ₂].	Andrés-Hernández et al. (2013)

HO_x concentrations in polluted or semi-polluted environments. Highlights from these studies are discussed here, with particular attention paid to those involving measurements of HO_x, NO₃, and O₃ and to those in which the contributions made by O₃ and NO₃ to night-time radical chemistry have been considered.

Geyer et al. (2003) report radical measurements and modelling from the 1998 Berlin Ozone Experiment (BERLIOZ). Measurements of NO₃, RO₂, HO₂, and OH were made by matrix isolation electron spin resonance (MIESR), chemical amplification (CA), and laser-induced fluorescence (LIF)

spectroscopy at a site approximately 50 km from Berlin. HO₂ was detected at night, with concentrations frequently as high as 5 × 10⁷ molecule cm⁻³ (approximately 2 pptv) and an average concentration of 1 × 10⁸ molecule cm⁻³ over 1 h (02:00 to 03:00) of nocturnal measurements during an intensive period of the study (Holland et al., 2003). OH was usually below the limit of detection of the LIF instrument (3.5 × 10⁵ molecule cm⁻³). Modelling revealed that nitrate radical reactions with terpenes were responsible for producing 53% of HO₂ and 36% of OH radicals in the night, with ozonolysis accounting for the production of the remaining

47 % of HO₂ and 64 % of OH radicals. A positive linear correlation between RO₂ and NO₃ was observed and was reproduced by the model.

Reactions of O₃ with alkenes were found to be responsible for the majority of the formation of OH during the winter PUMA (Pollution of the Urban Midlands Atmosphere) campaign (a low-photolysis urban environment) (Heard et al., 2004; Emmerson et al., 2005; Harrison et al., 2006). Measurements of OH, HO₂, and RO₂ were unavailable at night, but model-predicted values of these radicals were used to calculate that 90 % of night-time initiation via HO₂ was from O₃ reactions. Without measurements of NO₃ during the campaign, there was no estimate of its contribution to radical initiation.

Modelling results from the MCMA-2003 (Mexico City) field campaign (Volkamer et al., 2010) indicate that night-time radical production at roof-top level (approximately 16 m above the ground) was dominated by ozonolysis of alkenes, and that reactions of NO₃ with alkenes played only a minor role. The measurement site was located in a polluted urban environment, with high levels of NO, NO₂, and O₃. NO₃ was observed at a maximum concentration of 50 pptv during the night at a mean height above the ground of 70 m. Roof-top level concentrations of NO₃ were estimated using a linear scaling factor, calculated from the observed O₃ vertical gradient, and were found to be, on average, 3 times lower than the concentrations measured at 70 m. This predicted vertical gradient accounts for the relative unimportance of NO₃ reactions in radical initiation at roof-top level. The propagation of RO₂ radicals to HO₂ and OH, by reaction with NO₃, was found to be negligible.

The 2006 Texas Air Quality Study (TexAQS) involved a series of night-time flights onboard the NOAA P-3 aircraft over Houston, Texas, and along the Gulf Coast (Brown et al., 2011). Loss rates and budgets of NO₃ and highly reactive VOCs were calculated, but there were no measurements of OH, HO₂, and RO₂ during the flights. Budgets for NO₃ show that it was lost primarily through reactions with unsaturated VOCs, but the contribution to NO₃ loss through reaction with peroxy radicals was uncertain because of the lack of direct measurements of RO₂ during the flights. NO₃ dominated VOC oxidation, being 3 to 5 times more important than O₃.

In summary, NO₃ and O₃ have both been found to dominate radical initiation in the night-time troposphere, and in some situations the two mechanisms were found to be equally important. The relative importance of O₃- and NO₃-initiated oxidation depends on the availability of NO₃, which is determined by the amount of NO_x present in the atmosphere and the ratio of NO to NO₂, and on the concentration and species distribution of VOCs (Bey et al., 2001; Geyer et al., 2003). A modelling study by Bey et al. (2001) suggests that nocturnal radical initiation is driven by alkene ozonolysis in urban environments or in environments with low NO_x concentrations, while both O₃ and NO₃ contribute to radical

initiation in rural environments with moderate NO_x levels. It is expected that NO₃ dominates nocturnal radical initiation in air masses containing sufficient NO₂ and O₃ for NO₃ production while being deprived of NO (e.g. air masses downwind of urban areas). Geyer and Stutz (2004b) have found that the effects of suppressed mixing in the nocturnal boundary layer can also control whether NO₃ or O₃ dominates night-time radical chemistry.

In this paper we report airborne measurements of OH and HO₂ made during the RONOCO (ROLE of Nighttime chemistry in controlling the Oxidising Capacity of the atmosphere) and SeptEx (September Experiment) projects in 2010 and 2011. The rates of reaction between O₃, NO₃, and OH with the alkenes measured during the flights are investigated. The analysis of radical production from the night-time reactions of O₃ and NO₃ with alkenes is also given. Comparisons are made between the daytime and night-time chemistry studied and between the summer and winter measurement periods. Details and results of a box modelling study, and a comparison to the observations, are given by Stone et al. (2014b).

2 Details of the RONOCO and SeptEx fieldwork

RONOCO is a Natural Environment Research Council (NERC)-funded consortium project aimed at improving our understanding of the mechanisms and impact of nocturnal oxidation chemistry over the UK. The RONOCO fieldwork consisted of two measurement campaigns, in July 2010 and January 2011. Additional fieldwork, SeptEx, was conducted in September 2010. The RONOCO and SeptEx flights were conducted onboard the BAe-146 research aircraft operated by the Facility for Airborne Atmospheric Measurements (FAAM). Both field measurement campaigns were based at East Midlands Airport (52.8° N, 1.3° W) in the UK. During RONOCO the majority of the flying took place at night, with occasional flights beginning or ending in daylight hours to study chemical behaviour at dusk and dawn. Flights during SeptEx were mainly during the day, providing a useful comparison to the nocturnal chemistry.

Flights were conducted between altitudes of 50 and 6400 m, above the UK and the North Sea. Figure 1 shows the flight tracks during the summer, SeptEx, and winter measurements coloured by altitude. Measurements of OH and HO₂ were made using the University of Leeds aircraft-based fluorescence assay by gas expansion (FAGE) instrument. A suite of supporting measurements, including CO, O₃, NO, H₂O, VOCs, NO₃, and HCHO, were made during the flights and have been used in the current work. Table 2 summarises the techniques used to measure these species.

Air mass histories for each flight have been calculated using the UK Met Office Numerical Atmospheric-dispersion Modelling Environment (NAME). NAME is a three-dimensional Lagrangian particle dispersion model (Jones et al., 2007), which is run here using the UK Meteor-

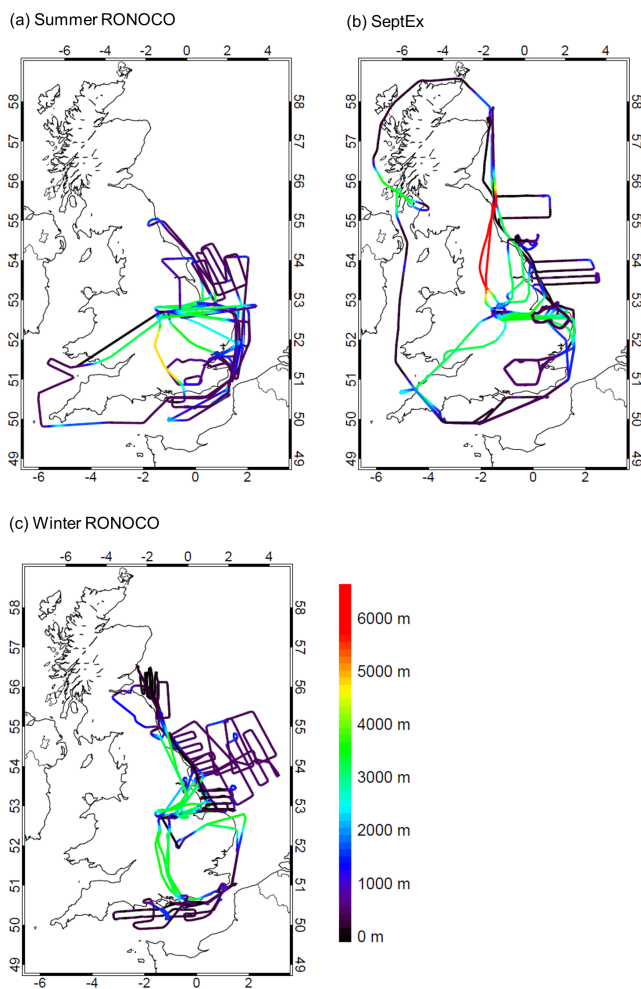


Figure 1. Flight tracks for (a) summer RONOCO, (b) SeptEx, and (c) winter RONOCO measurement campaigns, coloured by altitude.

logical Office's Unified Model meteorological fields. Model "particles", restricted to a 300 m deep layer from the surface, were released along the flight path and were tracked backwards through the modelled atmosphere. Model particle densities were integrated over 24 h periods, beginning at 24, 48, 72, and 96 h before each flight. The resulting "footprint" maps show the regions where the measured air has been in contact with the surface over the 4 days preceding a flight. An example is shown in Fig. 2, which shows model particle densities integrated over the 24 h period beginning 48 h prior to flight B535. The majority of the summer flights were characterised by air masses originating from the west and southwest of the UK, having Atlantic or continental European influences. The SeptEx flights were predominantly influenced by air masses from the north-east, east, and south-east of the UK, with northern European influences. The winter flights were mainly characterised by air masses arriving from the west of the UK, bringing Atlantic influences.

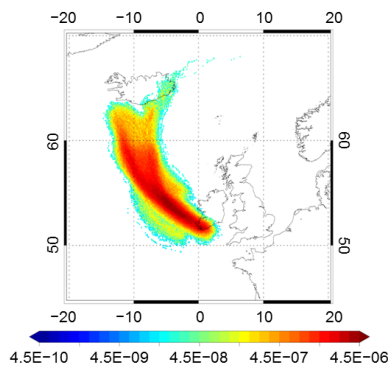


Figure 2. Footprint map for flight B535 on 17 July 2010, showing model particle densities (g s m^{-3}) in a 300 m deep layer from the surface, integrated over a 24 h period beginning 48 h prior to the flight.

Table 3 gives mean and maximum mixing ratios of CO, O₃, NO, and NO₂ measured during RONOCO and SeptEx. The mean mixing ratios of NO measured during the summer RONOCO flights are much lower than ground-based night-time measurements (e.g. 1.0 ppbv during the Tropospheric ORganic CHemistry experiment (TORCH) (Emmerson and Carslaw, 2009), 0–20 ppbv during the PM_{2.5} Technology Assessment and Characteristics Study-New York (PMTACS-NY); Ren et al., 2006) but are comparable with previous airborne night-time measurements (e.g. <30 pptv during the Texas Air Quality Study (TexAQS; Brown et al., 2011). Mean values of NO up to 14 pptv were reported by Salisbury et al. (2001) for semi-polluted air masses sampled at Mace Head. These comparisons indicate that the RONOCO and SeptEx flights enabled the sampling of air masses generally removed from the influence of NO in fresh surface emissions. Table 3 also highlights the unusual chemical conditions encountered during flight B537 on 20 July 2010, discussed further in Sect. 4.1. Night-time altitude profiles of NO₃, O₃, *trans*-2-butene, and propene (the latter two being illustrative of the alkenes measured) are given in Fig. 3.

3 Experimental

3.1 The Leeds FAGE aircraft instrument

The University of Leeds aircraft FAGE instrument has been described in detail by Commane et al. (2010). A brief description is given here. The instrument, which was designed specifically for use onboard the FAAM BAe-146 research aircraft (Floquet, 2006), is housed in two double-width 19 in. aircraft racks, with the inlet, detection cells, and pump set being separate from the two racks. Ambient air is sampled through a 0.7 mm diameter "pinhole" into a cylindrical inlet (length: 50 cm; diameter: 5 cm) which extends through a window blank on the starboard side of the aircraft.

Table 2. Details of supporting measurements.

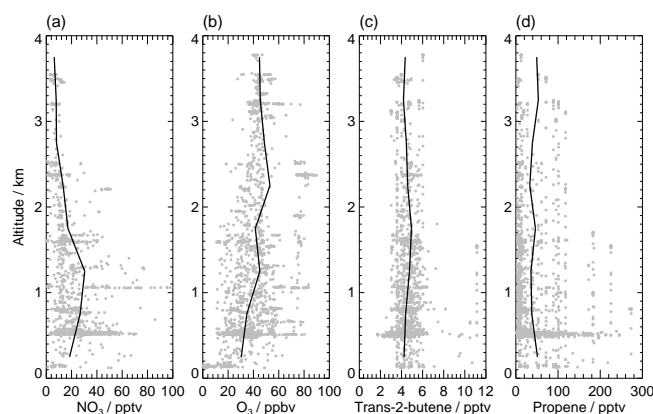
Species	Instrument, technique	Time resolution; limit of detection (LOD)	References
CO	Aero Laser AL5002 Fast Carbon Monoxide Monitor. Excitation and fast-response fluorescence at $\lambda = 150$ nm.	1 s; 3.5 ppbv	Gerbig et al. (1999)
O ₃	Thermo Scientific TEi49C ozone analyser. Absorption spectroscopy at $\lambda = 254$ nm.	1 s; 0.6 ppbv	Hewitt et al. (2010)
NO, NO ₂ , NO _x (NO + NO ₂)	Air Quality Design dual-channel fast-response NO _x instrument. Chemiluminescence from NO + O ₃ reaction. Conversion of NO ₂ to NO by photolysis.	10 s; 3 pptv for NO, 15 pptv for NO ₂	Stewart et al. (2008)
NO ₂ , Σ ANs, Σ PNs	TD-LIF (thermal dissociation laser-induced fluorescence). Detection of NO ₂ by laser-induced fluorescence. Thermal decomposition of Σ ANs (total alkyl nitrate) and Σ PNs (total peroxy nitrate) to NO ₂ .	1 s; 9.8 pptv for NO ₂ , 28.1 pptv for Σ ANs, 18.4 pptv for Σ PNs	Dari-Salisburgo et al. (2009); Di Carlo et al. (2013)
Alkenes	Whole air samples (WAS) analysed by laboratory-based gas chromatography with flame ionisation detection (GC-FID).	Typically 30 s; variable limits of detection	Hopkins et al. (2003)
NO ₃ , N ₂ O ₅	BBCEAS (broadband cavity-enhanced absorption spectroscopy) of NO ₃ at $\lambda = 642$ – 672 nm. N ₂ O ₅ measured following thermal dissociation to NO ₃ + NO ₂ .	1 s; 1.1 pptv for NO ₃ , 2.4 pptv for NO ₃ + N ₂ O ₅	Kennedy et al. (2011)
HCHO	Hantzsch technique: liquid-phase reaction of formaldehyde followed by excitation and fluorescence of resulting adduct at $\lambda = 510$ nm.	60 s; 81 pptv	Still et al. (2006)

Table 3. Mean mixing ratios of selected gas-phase species, and air temperature, measured during RONOCO and SeptEx. The flight and season during which the maximum values were measured are given in parentheses. NO₂ data are from the TD-LIF instrument. Zero values indicate measurements below the limit of detection.

Species	Summer RONOCO	SeptEx	Winter RONOCO	Maximum
CO/ppbv	102.3	117.1	139.3	256.0 (B537, summer)
O ₃ /ppbv	39.6	40.4	38.6	89.8 (B537, summer)
NO ₃ /pptv	21.1	0	6.2	176.9 (B537, summer)
NO/ppbv	0.05	0	0	18.9 (B539, summer)
NO ₂ /ppbv	1.6	1.7	2.3	18.6 (B568, winter)
Temperature/K	286.5	286.2	276.4	297.5 (B537, summer)

Downstream of the inlet are two low-pressure fluorescence cells positioned in series, the first for the detection of OH and the second for the detection of HO₂. During the RONOCO and SeptEx flights, the pressure inside the cells ranged from 1.9 Torr at ground level to 1.2 Torr at 6 km.

Laser light at $\lambda \sim 308$ nm is generated by a diode-pumped Nd:YAG-pumped tunable Ti:sapphire laser (Photonics Industries DS-532-10 and TU-UV-308 nm) and delivered to the fluorescence cells via optical fibres, on an axis perpendicular to the gas flow. A small fraction of the Ti:sapphire second harmonic ($\lambda = 462$ nm) is directed to the probe of a waveme-

**Figure 3.** Night-time altitude profiles of (a) NO₃; (b) O₃; (c) *trans*-2-butene; and (d) propene, showing 60 s data (grey points) and mean values in 500 m altitude bins (black lines).

ter to enable measurement of the laser wavelength to within 0.001 nm. A UV photodiode is positioned opposite the laser input arm on each fluorescence cell to measure laser power.

The sampled air forms a supersonic gas expansion beam in which the rate of collision between OH radicals and ambient air molecules is reduced. The OH fluorescence lifetime is

therefore extended to several hundred nanoseconds, significantly longer than the laser pulse, so that the measured signal can be temporally discriminated from laser scattered light. OH is excited from its ground state, X²Π_i (*v*' = 0), to its first electronically excited state, A²Σ⁺ (*v*' = 0), at λ ~ 308 nm. The resulting on-resonance fluorescence is detected by a UV-sensitive channel photomultiplier tube on an axis perpendicular to both the gas flow and the laser light. HO₂ is detected by titration with an excess of NO (Reaction R7), the resulting OH being detected as described.

The FAGE instrument was calibrated prior to and following each field measurement period, using a well-established method (Edwards et al., 2003; Faloona et al., 2004; Commane et al., 2010). Light at λ = 184.9 nm from a mercury pen-ray lamp photolyses water vapour in a flow of synthetic air inside an aluminium flow tube, generating OH and HO₂ at known concentrations. The aircraft FAGE instrument's limit of detection (LOD) for OH and HO₂ is determined by the instrument's sensitivity and the standard deviation of the background signal. During the RONOCO and SeptEx fieldwork, the 1σ LOD for a 5 min averaging period ranged between 0.64 and 1.8 × 10⁶ molecule cm⁻³ for OH and between 5.9 and 6.9 × 10⁵ molecule cm⁻³ for HO₂.

3.2 RO₂-based interference in FAGE measurements of HO₂

It has recently been shown that the reaction of alkene-derived β-hydroxyalkyl peroxy radicals, RO₂, with NO inside the HO₂ detection cell can lead to interference in FAGE HO₂ measurements (Fuchs et al., 2011; Whalley et al., 2013). The magnitude of the interference depends on the parent alkene, the residence time and mean temperature inside the cell, and the amount of NO injected. The interference therefore depends on the chemical environment and differs between FAGE instruments. In view of this, the University of Leeds ground-based and aircraft FAGE instruments have been tested for RO₂ interference. Thorough descriptions of the ground-based experimental method and results, and the results of a modelling study, are given by Whalley et al. (2013). The strongest interference in the aircraft instrument measurements was observed for ethene-derived RO₂, amounting to an increase of 39.7 ± 4.8 % in the observed HO₂ signal, with a cell pressure of 1.8 Torr, an estimated detection cell temperature of 255 K (obtained from rotational excitation spectra performed previously), and [NO]_{cell} = 10¹⁴ molecule cm⁻³.

Whalley et al. (2013) show that the chemistry responsible for the observed interferences is well known and that a model using the Master Chemical Mechanism (MCM, version 3.2: Jenkin et al., 1997; Saunders et al., 2003; Bloss et al., 2005, via <http://mcm.leeds.ac.uk/MCM>) can reproduce the interferences once tuned to the conversion efficiency of HO₂ to OH in the FAGE detection cell. Accordingly, Stone et al. (2014b) have applied the results of the ethene-derived RO₂ interference testing in a modelling study to assess the ef-

fect of the interference on the HO₂ measurements made during the RONOCO and SeptEx campaigns. A box model using a detailed MCM scheme was used to calculate a total potential interference in the RONOCO HO₂ measurements. The model was constrained to the conditions in the detection cell (1.8 Torr, 255 K, [NO] ~ 10¹⁴ molecule cm⁻³). Equal concentrations of HO₂ and ∑ RO₂ (sum of all peroxy radicals in the MCM generated from the parent hydrocarbon) were used to initialise the model. The model run time was varied until the model-predicted interference from ethene-derived RO₂ radicals was equal to the experimentally determined interference, thereby tuning the model to the conversion efficiency of HO₂ to OH. An interference factor, *f*, was calculated for each RO₂ in the MCM as follows:

$$f = \frac{[\text{OH}]_{\text{HO}_2+\text{RO}_2} - [\text{OH}]_{\text{HO}_2}}{[\text{OH}]_{\text{HO}_2}}, \quad (1)$$

where [OH]_{HO₂+RO₂} and [OH]_{HO₂} are the modelled concentrations of OH produced from the reactions of RO₂ and HO₂ and the concentration from HO₂ alone, respectively. The greatest interference was calculated to come from isoprene-derived peroxy radicals, followed by aromatic compounds and C₂ to C₅ alkenes. The smallest modelled interference is from the C₁ to C₃ alkanes. The interference factors were applied to model-predicted RO₂ speciation and concentrations for the RONOCO flights. Model-predicted RO₂ species were dominated by CH₃O₂ (33 %; *f* = 1.1 %) and HO₂ (24 %; *f* = 0.0 %), with smaller contributions from RO₂ derived from *iso*-butene (12 %; *f* = 0.5 %), *cis*-2-butene and *trans*-2-butene (10 %; *f* = 0.05 %), and isoprene (2 %; *f* = 7.6 %). RO₂ species with high interference factors were a minor component of the total RO₂. A modelled value of HO₂ including the total potential interference, HO₂^{*}, was calculated using

$$[\text{HO}_2^*] = [\text{HO}_2]_{\text{mod}} + \sum_i f_i [\text{RO}_{2,i}]_{\text{mod}}. \quad (2)$$

Direct comparison between modelled values of [HO₂^{*}] and the FAGE-measured values of [HO₂] was therefore made possible. The model-predicted interference during the RONOCO campaign is described by [HO₂^{*}] = 1.15 [HO₂] + 2 × 10⁵ molecule cm⁻³. The average model-predicted interference in the HO₂ measurements is 14 %. The HO₂ measurements made during RONOCO and SeptEx were not adjusted since speciated RO₂ measurements were not available. The measurements are hereafter referred to as HO₂^{*}.

The magnitude of the RO₂ interference can be reduced by lessening the concentration of NO in the detection cell. This also reduces the instrument sensitivity to HO₂. Since the conversion of RO₂ to OH requires at least two NO molecules, while the conversion of HO₂ requires only one molecule, the ratio of HO₂ signal to RO₂ signal can be made favourable by reducing [NO] (Whalley et al., 2013). This effect has been investigated for the ground-based instrument and will

be investigated for the aircraft instrument prior to future HO_x measurement campaigns. An overview of the laboratory and computational studies of the interference in different FAGE instruments is given in a recent review by Stone et al. (2012).

3.3 BBCEAS measurements of NO₃ and N₂O₅

NO₃ and N₂O₅ were measured by the University of Cambridge broadband cavity-enhanced absorption spectroscopy (BBCEAS) instrument. The instrument was designed and built specifically for the RONOCO project and is described in detail in Kennedy et al. (2011). A brief description is given here.

The instrument consists of three 94 cm long high-finesse optical cavities formed by pairs of highly reflecting mirrors. The cavities are irradiated by incoherent broadband continuous wave light sources. Two of the cavities, for the detection of N₂O₅ and NO₃, are irradiated by red light-emitting diodes (LEDs) centred at 660 nm. The third cavity, for the detection of NO₂, is irradiated by a blue LED centred at 460 nm. The light from the LEDs is collimated using optical fibres and a focussing lens at the input of each cavity. A spectrometer, consisting of a spectrograph and charge couple device (CCD), is positioned at the end of each cavity to measure the wavelength-dependent intensity of transmitted light.

Ambient air is sampled through a rear-facing inlet on the aircraft fuselage, positioned approximately 4 m from the aircraft nose and 10 cm from the aircraft body. The air from the inlet is divided into two flows. The flow directed to the N₂O₅ cavity is heated to 120 °C to ensure near complete (>99.6 %) thermal dissociation of N₂O₅ to NO₂ and NO₃. The cavity itself is heated to 80 °C and is used to measure the sum of the concentrations of ambient NO₃ plus NO₃ from thermal decomposition of N₂O₅. The second flow is unheated and is directed first through the NO₃ cavity and then through the NO₂ cavity. Background spectra are recorded at half-hour intervals during flights by halting the flow of ambient air and purging the cavities with nitrogen.

NO₃ is detected by its strong B²E' – X²A'₂ electronic transition centred at 662 nm. The concentration of NO₃ is determined by separating the finely structured NO₃ absorption features from the broad features caused by Rayleigh and Mie scattering using a fitting technique analogous to that employed in differential optical absorption spectroscopy (DOAS). A strong water vapour absorption feature that spectrally overlaps with NO₃ absorption around 662 nm is simulated for the pressure and temperature measured in the cavity and is removed from the measured absorption spectrum. The concentration of N₂O₅ is determined by subtracting the concentration of ambient NO₃ measured in the unheated cavity from the sum of the concentrations of ambient and dissociated NO₃ measured in the heated cavity.

Contributions to uncertainties in ambient measurements of NO₃ and N₂O₅, including wall losses of NO₃ and N₂O₅, temperature- and pressure-dependent absorption cross sec-

tions of NO₃ and H₂O, and the length of the cavity occupied by the sample, have been thoroughly investigated in laboratory experiments or addressed in the data analysis routine. In addition, wall losses of NO₃ and N₂O₅ were determined before and after each flight to account for changes in the surface properties of the inlet and detection cell walls, which were found to be negligible. The total uncertainty in the measured concentration of ambient NO₃ was 11 %. The uncertainty in the measured concentration of ambient N₂O₅ is determined for each individual ambient measurement, being dependent on the NO₃ / N₂O₅ ratio, and was on the order of 15 %. During RONOCO flights, the 1σ limits of detection for NO₃ and the sum of NO₃ + N₂O₅ were 1.1 and 2.4 pptv, respectively, for a 1 s integration time.

4 Overview of OH and HO₂* measurements

FAGE measurements were made on 16 flights during RONOCO and 9 flights during SeptEx. There was insufficient laser power during flights B534 to B536 in the summer campaign to measure both OH and HO₂* by dividing the laser light between the two cells. OH was therefore not measured during these flights. Low laser power throughout the summer fieldwork caused relatively high fluctuations in laser power overall and therefore higher background variability. This resulted in higher limits of detection for OH (1.8 × 10⁶ molecule cm⁻³) and HO₂* (6.9 × 10⁵ molecule cm⁻³).

Table 4 summarises the OH and HO₂* measurements during RONOCO and SeptEx and gives the instrument's average 1σ limit of detection for a 5 min averaging period. OH was not detected above the limit of detection during the summer or winter RONOCO flights, resulting in upper limits of 1.8 × 10⁶ and 6.4 × 10⁵ molecule cm⁻³ for mean summer and winter concentrations, respectively. These upper limit values are similar to previously reported night-time OH measurements (Geyer et al., 2003; Holland et al., 2003; Ren et al., 2003b; Emmerson and Carslaw, 2009). The mean daytime OH concentration during SeptEx was 1.8 × 10⁶ molecule cm⁻³, which was above the limit of detection. The mean HO₂* mixing ratio was highest during SeptEx (2.9 pptv) and was higher during summer (1.6 pptv) than during winter (0.7 pptv). The OH and HO₂* data sets for RONOCO and SeptEx are shown as altitude profiles in Figs. 4 and 5, respectively.

Table 5 gives the mean and maximum HO₂* mixing ratios at different times of day during summer, SeptEx, and winter. Dawn, day, dusk, and night are defined by the solar zenith angle as follows: dawn and dusk are between 90 and 102° and are distinguished by the time of day; day is between 0 and 90°; night is between 102 and 180°.

The mean dusk HO₂* mixing ratio in summer was higher than the mean night-time mixing ratio, suggesting that photochemical production was still active at dusk in summer. The reverse was true for the winter data, with the highest mean

Table 4. Combined daytime and night-time mean concentrations of OH and mean mixing ratios of HO₂^{*} with the FAGE instrument's average 1σ limits of detection for a 5 min averaging period during the RONOCO and SeptEx fieldwork.

	OH/molecule cm ⁻³		HO ₂ [*] /pptv	
	Mean concentration	Limit of detection	Mean mixing ratio	Limit of detection
Summer		1.8 × 10 ⁶	1.6	0.03
SeptEx	1.8 × 10 ⁶	1.2 × 10 ⁶	2.9	0.02
Winter		6.4 × 10 ⁵	0.7	0.02

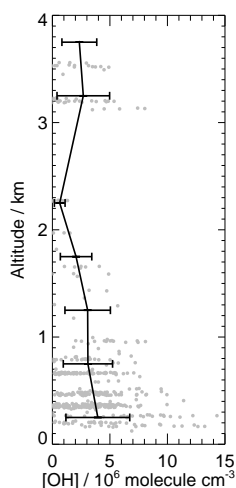


Figure 4. Altitude profile of OH measured during SeptEx showing 60 s data (grey points) and mean values in 500 m altitude bins (black lines). Error bars are 1 SD.

HO₂^{*} mixing ratio being at night. This suggests that when photochemical production was suppressed in the winter daytime due to low photolysis rates, production via reactions of NO₃ and O₃ with alkenes was an important route to radical initiation. The RONOCO HO₂^{*} measurements are similar to night-time, ground-based, urban measurements. For example, during the TORCH campaign, [HO₂] peaked at 1 × 10⁸ molecule cm⁻³ at night (Emmerson et al., 2007), and during the PMTACS-NY 2001 field campaign, night-time HO₂ concentrations of 8 × 10⁶ molecule cm⁻³ were measured (Ren et al., 2003b).

4.1 Case study flight B537: high night-time HO₂^{*} concentrations

The highest HO₂^{*} concentration (3.2 × 10⁷ molecule cm⁻³, 13.7 pptv) was measured during night-time flight B537 on 20 July 2010. Take-off from East Midlands Airport was at 22:00 local time (21:00 UTC, sunset at 20:18 UTC). The flight track, coloured by altitude, is shown in Fig. 6. The flight involved a profile descent from 3350 to 460 m down the Norfolk coast and a missed approach at Southend Air-

Table 5. Mean and, in parentheses, maximum HO₂^{*} mixing ratios measured during RONOCO and SeptEx.

	Mean (maximum) HO ₂ [*] mixing ratio/pptv		
	Summer	SeptEx	Winter
Dawn	0.74 (1.19)		0.54 (1.81)
Day		3.78 (11.79)	0.49 (1.68)
Dusk	2.73 (9.97)		0.32 (0.97)
Night	1.86 (13.58)		0.98 (2.02)

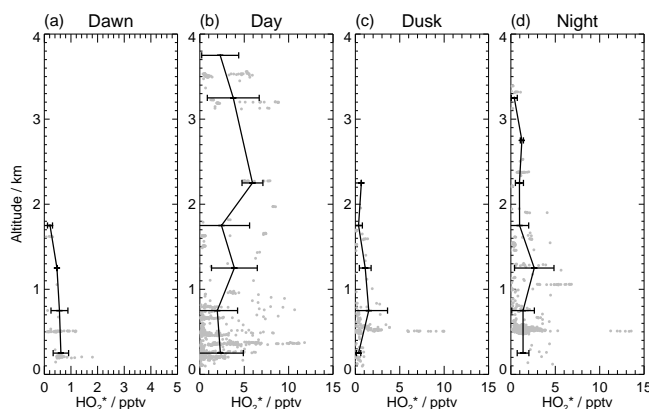


Figure 5. Altitude profiles of HO₂^{*} measured in RONOCO and SeptEx during (a) dawn; (b) day; (c) dusk; and (d) night, showing 60 s data (grey points) and mean values in 500 m altitude bins (black lines). Error bars are 1 SD.

port (51.6° N, 0.70° E). Plumes from European continental outflow (see Fig. 7) were intersected by a series of runs at altitudes between 460 m and the upper boundary of the polluted layer.

Flight B537 is an unusual flight within the RONOCO data set, with high concentrations of CO, O₃, NO₃, and high temperatures compared to the values measured during other night-time flights (see Table 3). The ambient aerosol surface area was significantly higher during B537 (nearly 800 μm² cm⁻³) than during other flights (between 100 and 400 μm² cm⁻³), and the organic aerosol concentration was significantly enhanced (Morgan et al., 2015). Footprint maps for flight B537, indicating regions where the sampled air was in contact with the surface prior to the flight, are shown in Fig. 7. The air sampled during the flight originated primarily over northern France, Belgium, and Germany.

A region of high surface pressure was positioned over the UK on the 20 July, with a mean air pressure of 1012.6 hPa over the 24 h prior to the flight. The mean air temperature 24 h prior to the flight (22:00, 19 July 2010, to 22:00, 20 July 2010), measured at a number of Met Office weather stations in Greater London, was 22.6 °C, and reached a maximum value of 28.6 °C. Wind speeds prior to the flight were low, with an average value of 4.7 knots (2.4 m s⁻¹). No rainfall was recorded at any of the Greater London weather sta-

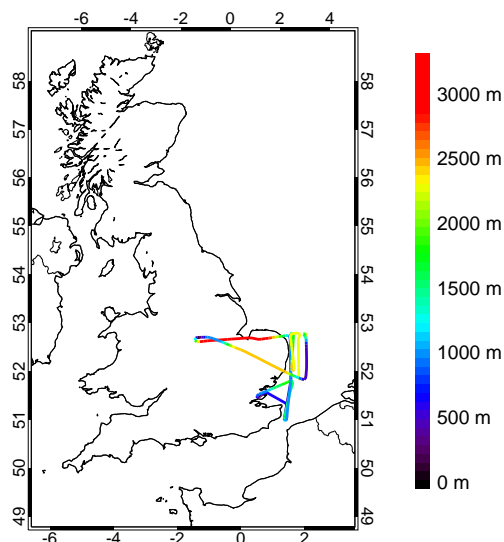


Figure 6. Flight track of flight B537 on 20 July 2010, coloured by altitude.

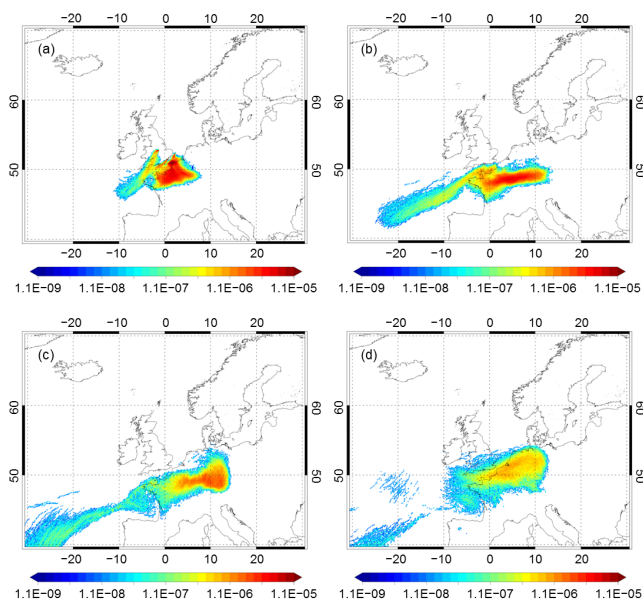


Figure 7. Footprint maps for flight B537 on 20 July 2010, showing model particle densities (g s m^{-3}) in a 300 m deep layer from the surface, integrated over 24 h periods beginning (a) 24 h, (b) 48 h, (c) 72 h, and (d) 96 h prior to the flight.

tions during the 24 h prior to the flight. At Heathrow Airport (51.5°N , 0.45°W), 12.4 h of sunshine were recorded on the 20 July. High temperatures, combined with low wind speed, exposure to solar radiation, and little precipitation promote the formation of ozone as a result of photochemical processing of VOCs emitted at the surface (e.g. Lee et al., 2006) and offer an explanation for the high ozone mixing ratios measured during flight B537. Peak surface daytime ozone concentrations measured in Teddington, London, on 20 July

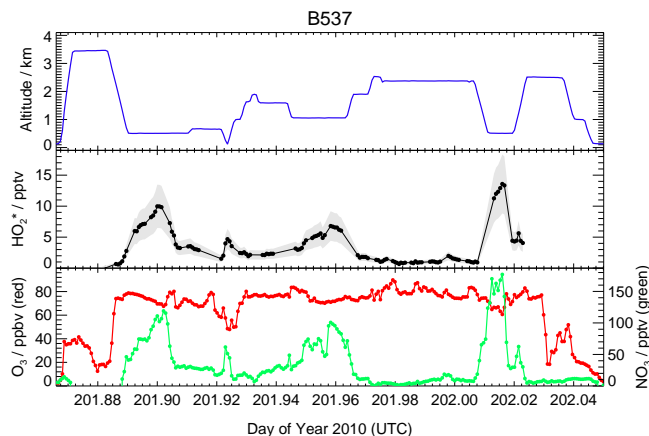


Figure 8. Time series of altitude (top panel, blue), HO₂^{*} (middle panel, black, with grey shading representing the uncertainty in the measurements), O₃ (bottom panel, red), and NO₃ (bottom panel, green) during night-time flight B537 on 20 July 2010.

were on the order of 2.0×10^{12} molecule cm^{-3} (~ 78 ppbv) (data available at <http://www.airquality.co.uk>). Similar levels were recorded at a number of locations within Greater London.

Figure 8 shows a time series of altitude, HO₂^{*}, O₃, and NO₃ mixing ratios during the flight, demonstrating very similar behaviour between the two radical species. During the missed approach at Southend Airport the mixing ratios of HO₂^{*} and NO₃ increased with decreasing altitude, to reach values of 4.5 and 35 pptv, respectively, at 50 m above the ground. The maximum HO₂^{*} and NO₃ mixing ratios were measured over the North Sea east of Ipswich (52.16°N , 2.34°E) at an altitude of 509 m, in the outflow of the London plume. Figure 9 shows scatter plots of HO₂^{*} against NO₃ and O₃ during flight B537 and during the other night-time flights during RONOCO. Strong positive correlation is evident between HO₂^{*} and NO₃ during B537 ($r = 0.97$), while during the remaining night flights there is still a significant, though weaker, correlation ($r = 0.58$). Moderate negative correlation is evident between HO₂^{*} and O₃ during B537 ($r = -0.46$), with weak positive correlation existing for the other night-time flights ($r = 0.19$). The data suggest that NO₃ was an important initiator of HO_x radicals during flight B537 and that O₃ played a limited role overall during the night-time flights. Further investigation of the roles of NO₃ and O₃ in alkene oxidation and radical initiation at night is described in Sect. 5.

5 Oxidation of alkenes and production of HO₂: method of analysis

Following the work of Salisbury et al. (2001), the total rates of reaction, Φ , of O₃ and NO₃ with the alkenes measured

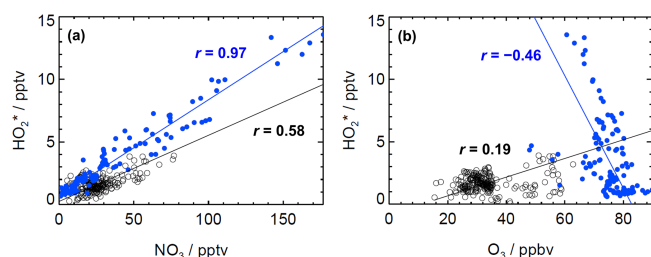


Figure 9. HO₂* vs. (a) NO₃ and (b) O₃ during flight B537 (blue, filled circles) and during all other night-time flights (black, open circles). The lines are lines of best fit to the data.

during RONOCO and SeptEx have been calculated:

$$\Phi_{\text{O}_3} = \sum_i^{\text{alkene}} k_{\text{O}_3+\text{alk}_i} [\text{O}_3][\text{alkene}_i] \quad (3)$$

$$\Phi_{\text{NO}_3} = \sum_i^{\text{alkene}} k_{\text{NO}_3+\text{alk}_i} [\text{NO}_3][\text{alkene}_i]. \quad (4)$$

The reactions of O₃ and NO₃ with alkenes yield OH, HO₂, and RO₂ radicals. A consideration of the reaction mechanisms of NO₃ and O₃ enables the calculation of the rate of instantaneous production of HO₂ (P_{HO_2}) from the reactions of NO₃ and O₃ with the alkenes measured during RONOCO, using the chemistry scheme, rate constants, and branching ratios in the MCM (Jenkin et al., 1997; Saunders et al., 2003).

Figure 10 shows a generalised reaction scheme for the reaction of NO₃ with an alkene. The reaction between NO₃ and an alkene proceeds via the addition of NO₃ to the double bond to form a nitrooxyalkyl radical, followed by rapid reaction with oxygen to yield a nitrooxyalkyl peroxy radical, RO₂ (shown as a single step in Fig. 10). The RO₂ radical can react with a number of species, of which NO, NO₃, and RO₂ lead to the production of an alkoxy radical (RO). Radical termination occurs via the reaction of RO₂ with HO₂ to yield a peroxide (ROOH) or with RO₂ to yield carbonyl (RC(O)CH₃) and alcohol (RCH₂OH) products. Reaction of RO with oxygen proceeds via the abstraction of a hydrogen atom to yield HO₂ or an aldehyde (RCHO). This generalised scheme can be applied to the reactions of NO₃ with all the alkenes measured. The rate of instantaneous production of HO₂ is found by first calculating the fraction of RO₂ that reacts to produce RO (F_{RO}) and the fraction of RO that reacts to produce HO₂ (F_{HO_2}):

$$F_{\text{RO}} = \frac{k_3 [\text{NO}] + k_4 [\text{NO}_3] + 0.6k_5 [\text{RO}_2]}{k_2 [\text{HO}_2] + k_3 [\text{NO}] + k_4 [\text{NO}_3] + k_5 [\text{RO}_2]} \quad (5)$$

$$F_{\text{HO}_2} = \frac{k_6 [\text{O}_2]}{k_7 + k_6 [\text{O}_2]}, \quad (6)$$

where RO₂ represents all peroxy radicals. Average values of F_{RO} for the NO₃+alkene reactions range between 0.50 for *trans*-2-pentene- and 1-pentene-derived RO₂ species and

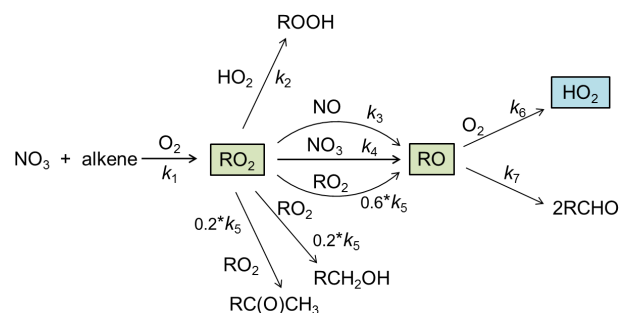


Figure 10. Generalised reaction scheme for production of RO₂ and HO₂ following reaction of NO₃ with an alkene.

0.61 for ethene-derived RO₂ species. F_{HO_2} varies between 0 and 1 for the alkenes studied. Overall, the rate of production of HO₂ (P_{HO_2}) from reactions of NO₃ with alkenes is then given by

$$P_{\text{HO}_2} = k_i [\text{NO}_3][\text{alkene}_i] \times F_{\text{RO}} \times F_{\text{HO}_2}. \quad (7)$$

The reaction scheme for the reaction of O₃ with alkenes is more complicated because the number and type of radicals produced in the O₃+alkene reaction depends on the structure of the alkene. The simplest case is the reaction of ozone with ethene. Ozone adds to the double bond to form a five-membered ring called a primary ozonide. Decomposition of the ozonide yields an excited Criegee intermediate (CH₂OO*) and a carbonyl compound (in this case formaldehyde, HCHO). The energy-rich Criegee intermediate can be stabilised by collision with a third body or undergo decomposition to yield products including OH, CO, and HO₂. The primary ozonide produced in the O₃+propene reaction (see Fig. 11) can decompose via two channels, yielding carbonyls and Criegee intermediates with different structures and different products, including RO₂. Reaction of RO₂ with NO, NO₃, and RO₂ (all peroxy radicals) yields RO, which in turn yields HO₂.

The rates of production of HO₂ from reactions of O₃ with alkenes (P_{HO_2}) have been calculated as follows:

$$P_{\text{HO}_2, \text{Direct}} = k_i [\text{O}_3][\text{alkene}_i] \times \alpha_{\text{HO}_2} \quad (8)$$

$$P_{\text{HO}_2, \text{RO}_2} = k_i [\text{O}_3][\text{alkene}_i] \times \alpha_{\text{RO}_2} \times F_{\text{RO}} \times F_{\text{HO}_2} \quad (9)$$

$$P_{\text{HO}_2} = P_{\text{HO}_2, \text{Direct}} + P_{\text{HO}_2, \text{RO}_2}, \quad (10)$$

where $P_{\text{HO}_2, \text{Direct}}$ is the rate of direct HO₂ production from Criegee intermediate decomposition, α_{HO_2} is the branching ratio to HO₂-producing channels from the Criegee intermediate, $P_{\text{HO}_2, \text{RO}_2}$ is the rate of HO₂ production from RO₂ radicals produced in the O₃+alkene reaction, α_{RO_2} is the branching ratio to RO₂-producing channels from the Criegee intermediate, F_{RO} is the fraction of RO₂ radicals that react to produce RO radicals, and F_{HO_2} is the fraction of RO radicals that react to produce HO₂ radicals, which is equal to 1 for all the alkenes studied. Average values of F_{RO} for

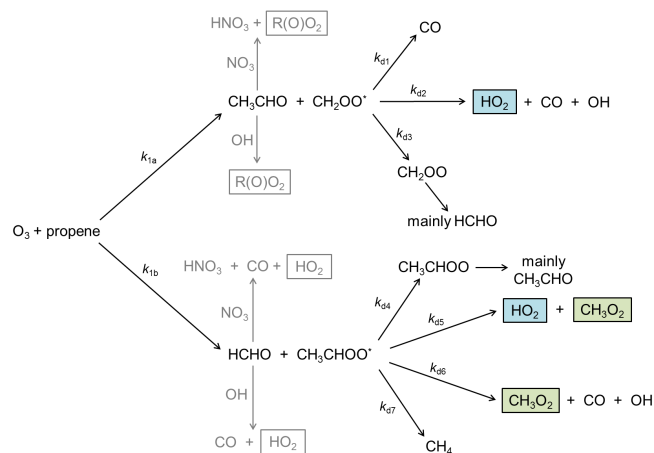


Figure 11. Reaction scheme for O₃ + propene, showing production of HO₂ and the methyl peroxy radical, CH₃O₂.

the O₃ + alkene reactions range between 0.54 for 1-pentene-derived RO₂ species and 0.64 for 1-butene- and *trans*-2-pentene-derived RO₂ species.

The reactions of RO₂ with NO to form RONO₂ have been omitted from the calculations because the branching ratio is small (0.001 to 0.02) for the radicals studied (Carter and Atkinson, 1989; Lightfoot et al., 1992). The reaction of CH₃O₂ with NO₂ to form CH₃O₂NO₂ has been omitted from the calculations, since the reverse reaction is much faster than the forward direction ($k_f = 6.4 \times 10^{-12} \text{ s}^{-1}$; $k_{\text{rev}} = 1.08 \text{ s}^{-1}$ at a mean temperature of 286.5 K during RONOCO).

The primary aims of the analysis presented here are three-fold: (1) to calculate the total rate of initiation through reactions of NO₃ and O₃ with alkenes; (2) to determine the relative importance of NO₃ and O₃ in night-time HO₂ production; (3) to investigate differences in radical production between different seasons and different times of day. The correlation between [HO₂]* and [NO₃], especially during flight B537, will be investigated.

P_{HO_2} has been calculated for each alkene measured for every 60 s data point where all the requisite data were available and where HO₂* was above the limit of detection of the FAGE instrument. Concentrations of RO₂ were calculated by scaling the observed HO₂* concentrations with the RO₂/HO₂* ratio calculated using a box model constrained to the concentrations of long-lived species measured during the flights (Stone et al., 2014b), i.e. $\text{RO}_{2,\text{obs}} = \text{HO}_{2^*,\text{obs}} \times \text{RO}_{2,\text{mod}} / \text{HO}_{2^*,\text{mod}}$. The rates of reaction and rates of production of HO₂ presented hereafter are average values for individual flights, seasons, or times of day.

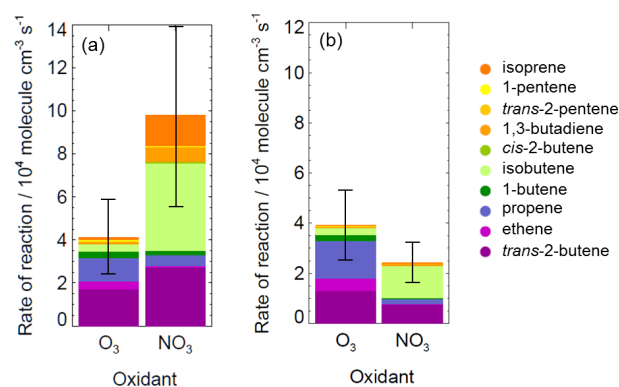


Figure 12. Average night-time rates of reaction between O₃ and NO₃ with alkenes during (a) summer and (b) winter RONOCO flights. Error bars represent the combined uncertainty in the measurements.

6 Results

6.1 Night-time oxidation of alkenes

Figure 12 shows histograms of the rate of reaction between O₃ and NO₃ with individual alkenes during summer and winter, for the night-time data only. The reactivity of measured alkenes ($\Phi_{\text{O}_3} + \Phi_{\text{NO}_3}$) was greater by a factor of 2.2 during summer flights than during winter flights. The reactions of NO₃ are largely responsible for this seasonal difference, since the contribution from O₃ + alkene reactions varies little between summer ($4.1 \times 10^4 \text{ molecule cm}^{-3} \text{ s}^{-1}$) and winter ($3.9 \times 10^4 \text{ molecule cm}^{-3} \text{ s}^{-1}$). The factor of 4.1 difference between the rate of NO₃ reactions in summer ($9.8 \times 10^4 \text{ molecule cm}^{-3} \text{ s}^{-1}$) and winter ($2.4 \times 10^4 \text{ molecule cm}^{-3} \text{ s}^{-1}$) can be attributed to the higher mean concentration of NO₃ in summer ($5.8 \times 10^8 \text{ molecule cm}^{-3}$) compared to winter ($2.0 \times 10^8 \text{ molecule cm}^{-3}$). This seasonal difference in NO₃ concentrations is attributable to the lower mean night-time temperature in winter (277.7 K) compared to summer (286.7 K), which disfavours NO₃ in the thermal equilibrium $\text{N}_2\text{O}_5 \rightleftharpoons \text{NO}_3 + \text{NO}_2$. $K_{\text{eq}}[\text{NO}_2]$, which determines $[\text{N}_2\text{O}_5] / [\text{NO}_3]$, is calculated to be 4.8 in summer and 29.6 in winter. At night in summer, Φ_{NO_3} was greater than Φ_{O_3} by a factor of 2.4, but in winter Φ_{O_3} was a factor of 1.6 greater than Φ_{NO_3} . Figure 12 illustrates the importance of the butene isomers (within the VOCs measured) in the reactions of O₃ and NO₃ and therefore radical initiation and propagation. Reactions with *iso*-butene dominated NO₃ reactivity in summer (42%) and winter (53%), with *trans*-2-butene also contributing significantly (28% in summer and 32% in winter). Reactions of O₃ were dominated by *trans*-2-butene (42% in summer and 34% in winter) and propene (26% in summer and 38% in winter). The importance of these alkenes is attributed to their relatively high abundances compared to the other alkenes measured,

Table 6. Average rates of instantaneous production of HO₂ from reactions of O₃ and NO₃ with alkenes.

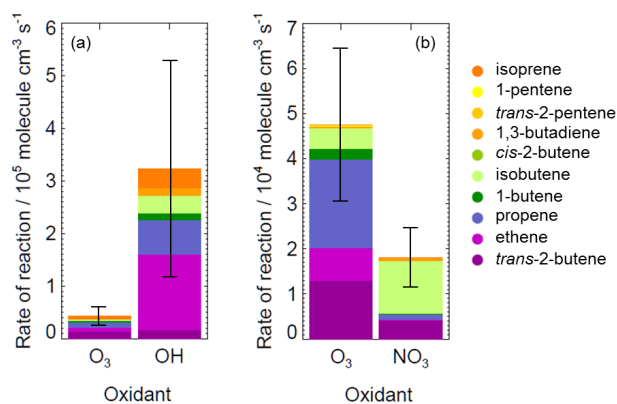
HO ₂ production rate (ΣP_{HO_2})/ 10 ⁴ molecule cm ⁻³ s ⁻¹				
	Dawn	Day	Dusk	Night
Summer				
NO ₃	0		2.8	3.8
O ₃	0.5		2.2	1.7
Total	0.5		5.0	5.5
Winter				
NO ₃	0.4	0.4	0.4	0.5
O ₃	1.4	1.5	1.2	1.2
Total	1.8	1.9	1.6	1.7

during both summer and winter, combined with their fast rates of reaction with O₃ and NO₃.

For comparison with the reactions of O₃ and NO₃, the total rate of reaction of measured alkenes with OH has been calculated using upper limits on OH concentrations of 1.8×10^6 molecule cm⁻³ and 6.4×10^5 molecule cm⁻³ for the summer and winter flights, respectively, based on the FAGE instrument's limit of detection. The high upper limits make the total rate of reaction of OH with alkenes, Φ_{OH} , unrealistically high for both summer (1.6×10^5 molecule cm⁻³ s⁻¹) and winter (7.8×10^4 molecule cm⁻³ s⁻¹). However, the OH reactivity will likely be considerably lower than the values calculated using the OH upper limits. A box model constrained to concentrations of long-lived species measured during the flights (Stone et al., 2014b) predicts a mean OH concentration of 2.4×10^4 molecule cm⁻³, significantly lower than the upper limits given by the instrument's limit of detection. Using the mean modelled value for OH gives $\Phi_{\text{OH}} = 2.1 \times 10^3$ molecule cm⁻³ s⁻¹ for summer and $\Phi_{\text{OH}} = 2.9 \times 10^3$ molecule cm⁻³ s⁻¹ for winter, indicating a diminished role for OH in alkene oxidation at night, in agreement with previous studies (e.g. Geyer et al., 2003; Emmerson et al., 2005).

6.2 Daytime oxidation of alkenes

Figure 13 shows histograms of rates of reaction of O₃ and OH with alkenes during SeptEx and of O₃ and NO₃ with alkenes during winter RONOCO flights, for daytime data only. OH was detected above the limit of detection (1.2×10^6 molecule cm⁻³) during the SeptEx flights, so the FAGE OH data were included in the calculations, using a reaction scheme analogous to the one shown in Fig. 10. NO₃ was not detected during the day in SeptEx. NO₃ is not expected to be present at measurable concentrations during daylight hours due to photolysis, but a mean con-

**Figure 13.** Average daytime rates of reaction of (a) O₃ and OH with alkenes during SeptEx and (b) O₃ and NO₃ with alkenes during winter. Note the different scales. NO₃ was not detected during daytime SeptEx flights (LOD = 1.1 pptv); OH was not detected during daytime winter flights (LOD = 6.4×10^5 molecule cm⁻³). Error bars represent the combined uncertainties in the measurements.

centration of 8.3×10^7 molecule cm⁻³ (3.3 pptv) was measured during the day in the winter RONOCO flights. These measurements of low mixing ratios of NO₃ may be partly caused by interference from other daytime species as observed by Brown et al. (2005) or by the variability in the instrument baseline, which can be on the order of 1–2 pptv during vertical profiles on the aircraft (Kennedy et al., 2011). This variability is small compared to the range of NO₃ values typically observed during RONOCO flights (0–50 pptv during summer; 0–10 pptv during winter). During SeptEx, Φ_{OH} exceeded Φ_{O_3} by a factor of 8. Ethene and propene were the two most abundant alkenes measured during SeptEx and contributed significantly to OH reactivity. O₃ reactivity with alkenes was dominated by propene and *trans*-2-butene (the six most abundant alkenes measured during SeptEx). NO₃ reactivity with alkenes was dominated by *trans*-2-butene and isobutene (the three most abundant alkene measured during winter daytime flights). The total rate of reaction of O₃ and OH with alkenes during daytime SeptEx flights (3.7×10^5 molecule cm⁻³ s⁻¹) exceeded the total rate of reaction of O₃ and NO₃ during daytime winter RONOCO flights (6.6×10^4 molecule cm⁻³ s⁻¹) by a factor of 6 and was more than double the total rate of reaction of O₃ and NO₃ with alkenes during night-time summer flights (1.4×10^5 molecule cm⁻³ s⁻¹). In winter daytime flights, Φ_{O_3} was greater than Φ_{NO_3} by a factor of 2.4.

Figures 12b and 13b reveal that reactions of O₃ dominated alkene reactivity during both daytime and night-time winter RONOCO flights. The concentrations of alkenes were generally higher at night, with the total alkene concentration (sum of concentrations of alkenes measured) being 2.1×10^9 molecule cm⁻³ in the day and 3.4×10^9 molecule cm⁻³ at night. The total measured alkene reactivity ($\Phi_{\text{O}_3} + \Phi_{\text{NO}_3}$) was marginally higher during the

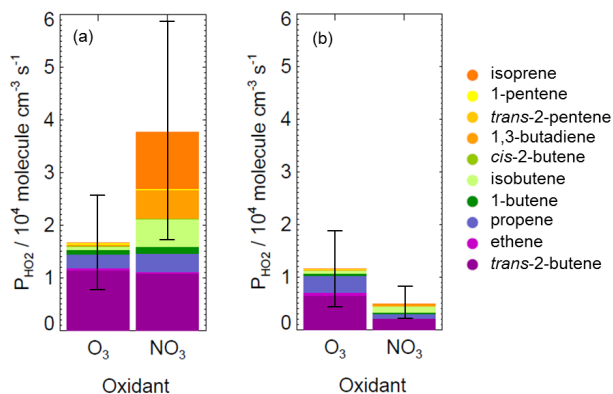


Figure 14. Average rates of instantaneous production of HO₂ from reactions of O₃ and NO₃ with alkenes during (a) summer and (b) winter RONOCO flights. Error bars represent the combined uncertainty in the measurements.

day, by a factor of 1.04. This difference is attributable mainly to the change in Φ_{O_3} .

Comparison of Figs. 12a and 13b reveals that the total measured alkene reactivity ($\Phi_{\text{O}_3} + \Phi_{\text{NO}_3}$) was higher during the summer night-time flights ($1.4 \times 10^5 \text{ molecule cm}^{-3} \text{ s}^{-1}$) than during the winter daytime flights ($6.6 \times 10^4 \text{ molecule cm}^{-3} \text{ s}^{-1}$), indicating a low oxidising environment during winter daytime. The additional contribution to measured alkene reactivity from reactions with OH has been calculated using the OH upper limits as described in Sect. 6.1. Even with this additional, upper-limit OH reactivity (1.6×10^5 and $1.1 \times 10^5 \text{ molecule cm}^{-3} \text{ s}^{-1}$ for summer night-time and winter daytime, respectively), the total summer night-time alkene reactivity remains higher than that during winter daytime, confirming the importance of the summer nocturnal troposphere for the oxidation of the measured alkenes.

6.3 Night-time production of HO₂ from reactions of O₃ and NO₃ with alkenes

Table 6 gives the total rates (ΣP_{HO_2}) of instantaneous production of HO₂ from the reactions of O₃ and NO₃ with alkenes. NO₃ was not detected during the dawn summer RONOCO flights, and there were no daytime RONOCO flights during summer. NO₃ dominated HO₂ production during dusk and night (68%), in agreement with Geyer et al. (2003), who found that NO₃ was responsible for 53% of HO₂ production at night in the BERLIOZ campaign. During winter, O₃ dominated HO₂ production at all times, with a night-time contribution of 70%. This is in agreement with the results from the winter PMTACS-NY 2004 field campaign (Ren et al., 2006).

The total rate of instantaneous production of HO₂ at night was 3.3 times greater in summer than in winter, with production from O₃ decreasing by a factor of 1.5 and produc-

tion from NO₃ decreasing by a factor of 7.8 between summer and winter. The mean temperature difference of 9 K between summer and winter is thought to be responsible for the lower NO₃ concentrations in winter ($2.0 \times 10^8 \text{ molecule cm}^{-3}$, 8.2 pptv, compared to $5.8 \times 10^8 \text{ molecule cm}^{-3}$, 24.5 pptv, in summer), owing to the increased thermal stability of N₂O₅, and for the reduced rate of temperature-dependent reactions between NO₃ and alkenes and subsequent reactions. There was very little difference between summer and winter mean O₃ mixing concentrations ($9.6 \times 10^{11} \text{ molecule cm}^{-3}$, 39.6 ppbv, and $9.4 \times 10^{11} \text{ molecule cm}^{-3}$, 38.6 ppbv, respectively).

The production of HO₂ via reactions of NO₃ and O₃ with alkenes is now examined in more detail. The rate of production from individual alkenes was calculated and plotted in a histogram, as shown in Fig. 14 for the summer and winter night-time data. During both summer and winter, reactions of O₃ and NO₃ with *trans*-2-butene were important sources of HO₂, contributing on average 62% to O₃-initiated HO₂ production and 36% to NO₃-initiated production during the summer and winter flights. Reactions of NO₃ with isoprene were important during summer, contributing 28% to NO₃-initiated production. The importance of *trans*-2-butene, despite its relatively low abundance during summer and winter night-time RONOCO flights (1.8 and 1.7 pptv, respectively, compared to ethene mixing ratios of 55.0 and 104.5 pptv), is attributed to its fast rates of reaction with both O₃ and NO₃ compared to the other alkenes measured. The importance of the isoprene + NO₃ reactions during the summer RONOCO flights is similarly attributed to its fast rate of reaction with NO₃ compared to the other alkenes measured. In addition there is no aldehyde-forming channel from the isoprene-derived RO radical (k_7 in Fig. 10), so that the yield of HO₂ from RO is equal to 1. The reaction of isobutene with NO₃ can proceed via one of two channels to produce two different RO₂ radicals but only one channel, with a branching ratio of 0.2, produces HO₂. Isobutene is therefore not a dominant contributor to HO₂ production, despite being the single largest contributor to NO₃ reactivity during daytime and night-time RONOCO flights (Figs. 12 and 13). Figure 14 highlights the small change in total production from O₃ between summer and winter and the dramatic change in total production from NO₃ between summer and winter.

Reactions of formaldehyde with NO₃ were included in the analysis where formaldehyde data were available (mean HCHO = 955 pptv). The NO₃ + HCHO reaction contributed a further $5.5 \times 10^3 \text{ molecule cm}^{-3} \text{ s}^{-1}$ (15%) to HO₂ production from NO₃ reactions, so that production from NO₃ contributed 79% of the total production.

6.4 Production of HO₂ during flight B537

Flight B537, on 20 July 2010, has been identified as an interesting flight, with high concentrations of HO₂* ($3.2 \times 10^8 \text{ molecule cm}^{-3}$; 13.6 pptv), ozone (peaking at

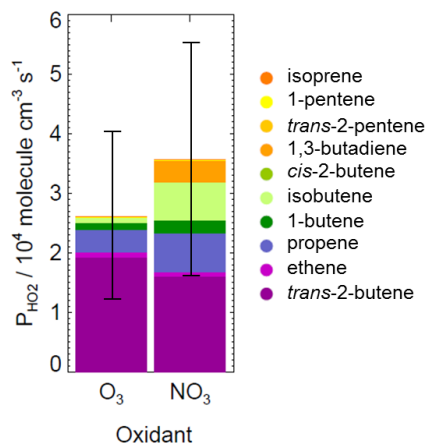


Figure 15. Average rates of instantaneous production of HO₂ from reactions of O₃ and NO₃ with alkenes during flight B537. Error bars represent the combined uncertainty in the measurements.

1.8×10^{12} molecule cm⁻³; 89.9 ppbv), and NO₃ (peaking at 4.1×10^9 molecule cm⁻³; 176.9 pptv), and a strong positive correlation between HO₂* and NO₃ ($r = 0.97$; see Fig. 9). NO, NO₂, and aerosol surface area were also elevated in-flight during flight B537 compared to their mean summer values. The highest concentration of ethene (1.43×10^{10} molecule cm⁻³; 0.61 ppbv) during the summer RONOCO flights was measured during B537. ΣP_{HO_2} from O₃ + alkene reactions (2.6×10^4 molecule cm⁻³ s⁻¹) was higher in flight B537 than in all the other summer flights, contributing 42 % of HO₂ production, with NO₃+alkene reactions contributing 3.6×10^4 molecule cm⁻³ (58 %). The total rate of HO₂ production from O₃ and NO₃ reactions during flight B537 was 6.2×10^4 molecule cm⁻³ s⁻¹. While this is higher than the average value of ΣP_{HO_2} for the summer flights (5.4×10^4 molecule cm⁻³ s⁻¹), it is not the highest rate of production during the summer flights. During B534 unusually high concentrations of isoprene, *cis*-2-butene, and 1,3-butadiene contributed to a total rate of HO₂ production of 7.9×10^4 molecule cm⁻³, which is the highest calculated value.

Figure 15 shows that the reactions of O₃ and NO₃ with *trans*-2-butene are once again important, contributing 74 % of $\Sigma P_{\text{HO}_2, \text{O}_3}$ and 45 % of $\Sigma P_{\text{HO}_2, \text{NO}_3}$. The correlation between HO₂* and NO₃ is attributed to the production of HO₂ by reactions of NO₃ with alkenes, especially *trans*-2-butene. Figure 16 shows HO₂* vs. the total instantaneous rate of production from the reactions of O₃ and NO₃ with alkenes during flight B537 at each 60 s data point during the flight for which the requisite data were available. Note that the rates plotted in Fig. 16 are higher than those shown in Fig. 15, where the rates of production of HO₂ from each alkene have been averaged across the whole flight. A strong positive correlation exists between HO₂* and both $\Sigma P_{\text{HO}_2, \text{O}_3}$ ($r = 0.6$)

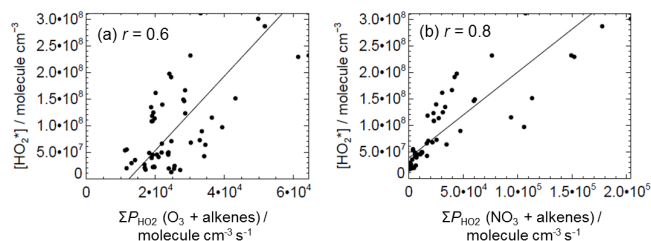


Figure 16. [HO₂*] vs. total rate of instantaneous production of HO₂ from reactions of (a) O₃ and (b) NO₃ during flight B537. Correlation coefficients (r) are given in each plot. The lines are lines of best fit to the data.

and $\Sigma P_{\text{HO}_2, \text{NO}_3}$ ($r = 0.8$), indicating the importance of these reactions for the production of HO₂ during this flight.

7 Comparison with model results

The observations of OH, HO₂*, NO₃, and N₂O₅ have been interpreted in the context of night-time oxidation chemistry using a box model constrained to observations of VOCs, NO_x, O₃, CO, and other long-lived species measured during the RONOCO flights (Stone et al., 2014b). The Dynamically Simple Model of Atmospheric Chemical Complexity (DSMACC) (Emmerson and Evans, 2009; Stone et al., 2010, 2014b) was initiated with concentrations of measured species, using a chemistry scheme based on the Master Chemical Mechanism (MCM, version 3.2: Jenkin et al., 1997, 2003; Saunders et al., 2003; Bloss et al., 2005, via <http://mcm.leeds.ac.uk/MCM>), and was allowed to run to diurnal steady state. The model output includes concentrations of OH, HO₂, NO₃, RO₂, and other species. Data from daytime flights, or during dawn or dusk periods, were not included in the model analysis. Data from flight B537 were also excluded, owing to the atypical observations of HO₂*, NO₃, O₃, and other chemical species made during this flight. The modelling study and results are described in more detail by Stone et al. (2014b).

The model predicts a mean OH concentration of 2.4×10^4 molecule cm⁻³ for the summer flights, which is consistent with the measured OH concentrations for which the instrument's limit of detection is an upper limit only. The base model underpredicts HO₂* by around 200 % and overpredicts NO₃ and N₂O₅ by 80 and 50 %, respectively. These discrepancies were investigated by determining the processes controlling radical production and loss in the model and using those results to improve model performance. Model production of HO₂ is dominated by reactions of RO + O₂ (42 %), with a significant contribution from OH + CO (31 %) despite low OH concentrations at night. RO_x (= RO + RO₂ + OH + HO₂) radical initiation in the model is dominated by reactions of NO₃ with unsaturated VOCs (80 %), with a much smaller contribution (18 %) from

alkene ozonolysis. Modelled HO₂ loss is dominated by its reactions with NO₃ (45 %) and O₃ (27 %), both of which are radical propagating routes and which are the dominant routes to OH production in the model. In fact NO₃ was found to control both radical initiation and propagation in the model.

These results are in general agreement with the results of the analysis presented in Sect. 6.1, though the model predicts a more important role for NO₃ (80 % of RO_x radical production, which is 7.2 times the contribution from O₃+alkenes) than is predicted by the analysis based on the observations alone (69 % of HO₂ radical production during summer, which is 2.1 times the contribution from O₃+alkenes). The model predicts a relatively small role for O₃ in both summer and winter. The model is constrained to measured values of O₃ but overpredicts NO₃. The mean measured NO₃ night-time mixing ratio was 24.5 pptv in the summer and 8.2 pptv in the winter. The mean modelled summer and winter values are 37.4 and 20.7 pptv, respectively. This discrepancy between modelled and measured NO₃ helps to explain the model overprediction of the role of NO₃ in HO_x radical initiation during the RONOCO flights. Modelled NO₃ reactivity was dominated by *iso*-butene (36 %) and *trans*-2-butene (27 %), and modelled O₃ reactivity was dominated by *trans*-2-butene (51 %), in agreement with the night-time alkene reactivities presented in Sect. 6.1.

An improvement to the model predictions of NO₃, N₂O₅, and HO₂^{*} was made by increasing the concentration of unsaturated VOCs in the model. Increasing the total observed alkene concentration by 4 times resulted in a modelled-to-observed ratio of 1.0 for HO₂^{*} and of ~1.2 for NO₃ and N₂O₅. Two-dimensional gas chromatography (GC × GC) analysis of the whole-air samples taken during RONOCO has revealed a large number of VOCs extra to those routinely measured (Lidster et al., 2014). Calibration standards for the majority of these species are not yet available, and so the quantification of their concentrations is not possible, but their detection confirms that the model overprediction of NO₃ and underprediction of HO₂^{*} are attributable to reactions of NO₃ with unquantified unsaturated hydrocarbons.

The presence of unquantified unsaturated VOCs during the RONOCO campaign, suggested by the model and confirmed by the two-dimensional GC analysis, has implications for the conclusions drawn from the analysis based on the observations. The relative contributions of NO₃ and O₃ to night-time radical initiation will change with the composition of unsaturated VOCs in the sampled air, due to the different rates of reaction of NO₃ and O₃ with different VOC species and the rates of production of HO₂ following these reactions. The model results indicate that the reaction of NO₃ with the unquantified VOCs leads to increased production of HO₂. The role of NO₃ in night-time radical production would therefore be enhanced by the inclusion of the unquantified VOCs in the observational analysis.

8 Conclusions

Night-time radical chemistry has been studied as part of the RONOCO and SeptEx campaigns onboard the BAe-146 research aircraft during summer 2010 and winter 2011. NO₃, N₂O₅, OH, and HO₂^{*} were measured simultaneously for the first time from an aircraft, with OH and HO₂^{*} being measured by the University of Leeds aircraft FAGE instrument. OH was detected above the limit of detection during the daytime SeptEx flights only, with a mean concentration of 1.8×10^6 molecule cm⁻³. Upper limits of 1.8×10^6 and 6.4×10^5 molecule cm⁻³ are placed on mean OH concentrations for the summer and winter RONOCO (night, dawn, and dusk) measurement campaigns, respectively. HO₂^{*} was detected above the limit of detection during the summer and winter RONOCO flights and during SeptEx, with a maximum mixing ratio of 13.6 pptv measured during the night-time flight B537 on 20 July 2010. Mean night-time HO₂^{*} mixing ratios were significantly higher in summer than in winter. Significant concentrations (up to 176.9 pptv) of NO₃ were measured during night-time flights, since the air masses sampled were sufficiently removed from the surface that the loss of NO₃ by reaction with NO was minimised. The RONOCO flights were therefore an excellent opportunity to study the role of NO₃ in nocturnal oxidation and radical initiation.

The rates of reaction of O₃ and NO₃ with the alkenes measured have been calculated. At night during summer, NO₃ dominated alkene reactivity. Several previous night-time studies have also found NO₃ to be the dominant nocturnal oxidant (e.g. Geyer et al., 2003; Brown et al., 2011). During night-time winter RONOCO flights the total rate of reaction of NO₃ with alkenes was much reduced, but the rate of reaction of O₃ with alkenes was similar to that in summer. During day and night in winter, O₃+alkene reactions were faster than NO₃+alkene reactions. Overall, during RONOCO, the combined rate of alkene oxidation by O₃ and NO₃ was highest at night during summer.

The calculation of the rates of the instantaneous production of HO₂ from reactions of O₃ and NO₃ with alkenes, using measurements made during the flights, has revealed that night-time production was dominated by NO₃ in summer and by O₃ in winter. The rate of instantaneous production of HO₂ from reactions of NO₃ with alkenes decreased significantly from summer to winter (87 %), whereas production from O₃+alkene reactions was similar in summer and winter, decreasing by just 31 %. Strong positive correlation between HO₂^{*} and NO₃, especially during flight B537, is attributed to the production of HO₂ from reactions of NO₃ with alkenes, particularly *trans*-2-butene and other isomers of butene.

Significant concentrations of HO₂^{*} were detected at night, with the highest HO₂^{*} concentration (13.6 pptv) being measured during a summer night-time flight, indicating that HO_x radical chemistry remains active at night under the right con-

ditions. The role of HO_x is diminished in the low photolysis winter daytime atmosphere, with alkene ozonolysis being primarily responsible for oxidation and radical initiation, in agreement with previous studies (e.g. Heard et al., 2004; Emmerson et al., 2005). Both the analysis presented here and the results of the box modelling study by Stone et al. (2014b) indicate that in air masses removed from sources of NO, NO₃ plays an important role in the oxidation of alkenes and radical initiation at night, in agreement with previous studies (e.g. Brown et al., 2011). Alkene ozonolysis also plays a significant role in nocturnal oxidation in agreement with Salisbury et al. (2001), Geyer et al. (2003), Ren et al. (2003a, 2006), Emmerson et al. (2005), and Volkamer et al. (2010). The balance between the roles of NO₃ and O₃ was controlled in part by [NO₃], with colder winter temperatures forcing the NO₃–N₂O₅ equilibrium towards N₂O₅.

The total rate of reaction of O₃ and NO₃ with alkenes during night-time summer flights (1.4×10^5 molecule cm⁻³ s⁻¹) was higher by a factor of 2.1 than during daytime winter flights (6.6×10^4 molecule cm⁻³ s⁻¹). Whilst it should be remembered that measurements at different times of day and in different seasons reflect composition changes in air masses (such as the abundance of reactive alkenes), this result supports the hypothesis that oxidation of certain VOCs, in particular the reactive alkenes, in the nocturnal summer atmosphere can be as rapid as in the winter daytime atmosphere.

A box model of night-time chemistry constrained to measurements of long-lived species has been used to investigate the night-time chemistry sampled during RONOCO (Stone et al., 2014b). The base model underpredicts HO₂* and overpredicts NO₃. These discrepancies were minimised by increasing the concentration of alkenes in the model, thereby increasing the reaction of NO₃ with alkenes and the production of HO₂. The presence of unquantified unsaturated VOCs has been confirmed by 2D-GC analysis, though the exact nature and concentrations of the ‘missing’ species are unclear. The inclusion of these species in the analysis presented in this paper would likely increase the role of NO₃ in the oxidation of alkenes and production of HO₂ at night.

Acknowledgements. This work was funded by the UK Natural Environment Research Council (NE/F004664/1). The authors would like to thank ground staff, engineers, scientists, and pilots involved in RONOCO for making this project a success. Airborne data were obtained using the BAe 146-301 Atmospheric Research Aircraft (ARA) flown by Directflight Ltd. and managed by the Facility for Airborne Atmospheric Measurements (FAAM), which is a joint entity of the Natural Environment Research Council (NERC) and the Met Office.

Edited by: S. Brown

References

- Andrés-Hernández, M. D., Kartal, D., Crowley, J. N., Sinha, V., Regelin, E., Martínez-Harder, M., Nenakhov, V., Williams, J., Harder, H., Bozem, H., Song, W., Thieser, J., Tang, M. J., Hosaynali Beigi, Z., and Burrows, J. P.: Diel peroxy radicals in a semi-industrial coastal area: nighttime formation of free radicals, *Atmos. Chem. Phys.*, 13, 5731–5749, doi:10.5194/acp-13-5731-2013, 2013.
- Atkinson, R. and Arey, J.: Gas-phase tropospheric chemistry of biogenic volatile organic compounds: a review, *Atmos. Environ.*, 37, 197–219, 2003.
- Beames, J. M., Liu, F., Lu, L., and Lester, M. I.: Ultraviolet Spectrum and Photochemistry of the Simplest Criegee Intermediate CH₂OO, *J. Am. Chem. Soc.*, 134, 20045–20048, 2012.
- Beames, J. M., Liu, F., Lu, L., and Lester, M. I.: UV spectroscopic characterization of an alkyl substituted Criegee intermediate CH₃CHOO, *J. Chem. Phys.*, 138, 244307, doi:10.1063/1.4810865, 2013.
- Berndt, T. and Böge, O.: Kinetics of Oxirane Formation in the Reaction of Nitrate Radicals with Tetramethylethylene, *Berichte der Bunsengesellschaft für physikalische Chemie*, 98, 869–871, 1994.
- Bey, I., Aumont, B., and Toupance, G.: A modeling study of the nighttime radical chemistry in the lower continental troposphere, *J. Geophys. Res.-Atmos.*, 106, 9991–10001, 2001.
- Bloss, C., Wagner, V., Bonzanini, A., Jenkin, M. E., Wirtz, K., Martin-Reviejo, M., and Pilling, M. J.: Evaluation of detailed aromatic mechanisms (MCMv3 and MCMv3.1) against environmental chamber data, *Atmos. Chem. Phys.*, 5, 623–639, doi:10.5194/acp-5-623-2005, 2005.
- Brown, S. S. and Stutz, J.: Nighttime radical observations and chemistry, *Chem. Soc. Rev.*, 41, 6405–6447, 2012.
- Brown, S. S., Dibb, J. E., Stark, H., Aldener, M., Vozella, M., Whitlow, S., Williams, E. J., Lerner, B. M., Jakoubek, R., Middlebrook, A. M., DeGouw, J. A., Warneke, C., Goldan, P. D., Kuster, W. C., Angevine, W. M., Sueper, D. T., Quinn, P. K., Bates, T. S., Meagher, J. F., Fehsenfeld, F. C., and Ravishankara, A. R.: Nighttime removal of NO_x in the summer marine boundary layer, *Geophys. Res. Lett.*, 31, L07108–L07113, 2004.
- Brown, S. S., Osthoff, H. D., Stark, H., Dubé, W. P., Ryerson, T. B., Warneke, C., de Gouw, J. A., Wollny, A. G., Parrish, D. D., Fehsenfeld, F. C., Ravishankara, A. R.: Aircraft observations of daytime NO₃ and N₂O₅ and their implications for tropospheric chemistry, *J. Photoch. Photobio. A*, 176, 270–278, 2005.
- Brown, S. S., Ryerson, T. B., Wollny, A. G., Brock, C. A., Peltier, R., Sullivan, A. P., Weber, R. J., Dubé, W. P., Trainer, M., Meagher, J. F., Fehsenfeld, F. C., and Ravishankara, A. R.: Variability in Nocturnal Nitrogen Oxide Processing and Its Role in Regional Air Quality, *Science*, 311, 67–70, 2006.
- Brown, S. S., Dubé, W. P., Peischl, J., Ryerson, T., Atlas, E., Warneke, C., de Gouw, J. A., te Lintel Hekkert, S., Brock, C. A., Flocke, F., Trainer, M., Parrish, D. D., Fehsenfeld, F. C., and Ravishankara, A.: Budgets for nocturnal VOC oxidation by nitrate radicals aloft during the 2006 Texas Air Quality Study, *J. Geophys. Res.-Atmos.*, 116, D24305–D24320, 2011.
- Carter, W. P. L. and Atkinson, R.: Alkyl Nitrate Formation from the Atmospheric Photooxidation of Alkanes; a Revised Estimation Method, *J. Atmos. Chem.*, 8, 165–173, 1989.

- Commane, R., Floquet, C. F. A., Ingham, T., Stone, D., Evans, M. J., and Heard, D. E.: Observations of OH and HO₂ radicals over West Africa, *Atmos. Chem. Phys.*, 10, 8783–8801, doi:10.5194/acp-10-8783-2010, 2010.
- Creasey, D. J., Heard, D. E., and Lee, J. D.: Eastern Atlantic Spring Experiment 1997 (EASE97) 1. Measurements of OH and HO₂ concentrations at Mace Head, Ireland, *J. Geophys. Res.-Atmos.*, 107, 4091–4106, 2002.
- Dari-Salisburgo, C., Di Carlo, P., Giammaria, F., Kajii, Y., and D'Altorio, A.: Laser induced fluorescence instrument for NO₂ measurements: Observations at a central Italy background site, *Atmos. Environ.*, 43, 970–977, 2009.
- Di Carlo, P., Aruffo, E., Busilacchio, M., Giammaria, F., Dari-Salisburgo, C., Biancofiore, F., Visconti, G., Lee, J., Moller, S., Reeves, C. E., Bauguitte, S., Forster, G., Jones, R. L., and Ouyang, B.: Aircraft based four-channel thermal dissociation laser induced fluorescence instrument for simultaneous measurements of NO₂, total peroxy nitrate, total alkyl nitrate, and HNO₃, *Atmos. Meas. Tech.*, 6, 971–980, doi:10.5194/amt-6-971-2013, 2013.
- Donahue, N. M., Kroll, J. H., Anderson, J. G., and Demerjian, K. L.: Direct observation of OH production from the ozonolysis of olefins, *Geophys. Res. Lett.*, 25, 59–62, 1998.
- Donahue, N. M., Drozd, G. T., Epstein, S. A., Presto, A. A., and Kroll, J. H.: Adventures in ozoneland: down the rabbit-hole, *Phys. Chem. Chem. Phys.*, 13, 10848–10857, 2011.
- Drozd, G. T. and Donahue, N. M.: Pressure Dependence of Stabilized Criegee Intermediate Formation from a Sequence of Alkenes, *J. Phys. Chem. A*, 115, 4381–4387, 2011.
- Edwards, G. D., Cantrell, C., Stephens, S., Hill, B., Goyea, O., Shetter, R., Mauldin, R. L., Kosciuch, E., Tanner, D., and Eisele, F.: Chemical Ionization Mass Spectrometer Instrument for the Measurement of Tropospheric HO₂ and RO₂, *Anal. Chem.*, 75, 5317–5327, 2003.
- Emmerson, K. M. and Carslaw, N.: Night-time radical chemistry during the TORCH campaign, *Atmos. Environ.*, 43, 3220–3226, 2009.
- Emmerson, K. M. and Evans, M. J.: Comparison of tropospheric gas-phase chemistry schemes for use within global models, *Atmos. Chem. Phys.*, 9, 1831–1845, doi:10.5194/acp-9-1831-2009, 2009.
- Emmerson, K. M., Carslaw, N., and Pilling, M. J.: Urban Atmospheric Chemistry During the PUMA Campaign 2: Radical Budgets for OH, HO₂ and RO₂, *J. Atmos. Chem.*, 52, 165–183, 2005.
- Emmerson, K. M., Carslaw, N., Carslaw, D. C., Lee, J. D., McFiggans, G., Bloss, W. J., Gravestock, T., Heard, D. E., Hopkins, J., Ingham, T., Pilling, M. J., Smith, S. C., Jacob, M., and Monks, P. S.: Free radical modelling studies during the UK TORCH Campaign in Summer 2003, *Atmos. Chem. Phys.*, 7, 167–181, doi:10.5194/acp-7-167-2007, 2007.
- Faloon, I. C., Tan, D., Leshner, R. L., Hazen, N. L., Frame, C. L., Simpas, J. B., Harder, H., Martinez, M., di Carlo, P., Ren, X., and Brune, W. H.: A Laser-Induced Fluorescence Instrument for Detecting Tropospheric OH and HO₂: Characteristics and Calibration, *J. Atmos. Chem.*, 47, 139–167, 2004.
- Fleming, Z. L., Monks, P. S., Rickard, A. R., Heard, D. E., Bloss, W. J., Seakins, P. W., Still, T. J., Sommariva, R., Pilling, M. J., Morgan, R., Green, T. J., Brough, N., Mills, G. P., Penkett, S. A., Lewis, A. C., Lee, J. D., Saiz-Lopez, A., and Plane, J. M. C.: Peroxy radical chemistry and the control of ozone photochemistry at Mace Head, Ireland during the summer of 2002, *Atmos. Chem. Phys.*, 6, 2193–2214, doi:10.5194/acp-6-2193-2006, 2006.
- Floquet, C. F. A.: Airborne Measurements of Hydroxyl Radicals by Fluorescence Assay by Gas Expansion, PhD, School of Chemistry, University of Leeds, Leeds, 155 pp., 2006.
- Fuchs, H., Bohn, B., Hofzumahaus, A., Holland, F., Lu, K. D., Nehr, S., Rohrer, F., and Wahner, A.: Detection of HO₂ by laser-induced fluorescence: calibration and interferences from RO₂ radicals, *Atmos. Meas. Tech.*, 4, 1209–1225, doi:10.5194/amt-4-1209-2011, 2011.
- Gerbig, C., Schmitgen, S., Kley, D., and Volz-Thomas, A.: An improved fast-response vacuum-UV resonance fluorescence CO instrument, *J. Geophys. Res.-Atmos.*, 104, 1699–1704, 1999.
- Geyer, A. and Stutz, J.: The vertical structure of OH-HO₂-RO₂ chemistry in the nocturnal boundary layer: A one-dimensional model study, *J. Geophys. Res.-Atmos.*, 109, D16301–D16316, 2004a.
- Geyer, A. and Stutz, J.: Vertical profiles of NO₃, N₂O₅, O₃, and NO_x in the nocturnal boundary layer: 2. Model studies on the altitude dependence of composition and chemistry, *J. Geophys. Res.-Atmos.*, 109, D12307, doi:10.1029/2003JD004211, 2004b.
- Geyer, A., Bächmann, K., Hofzumahaus, A., Holland, F., Konrad, S., Klüpfel, T., Pätz, H.-W., Perner, D., Mihelcic, D., Schäfer, H.-J., Volz-Thomas, A., and Platt, U.: Nighttime formation of peroxy and hydroxyl radicals during the BERLIOZ campaign: Observations and modeling studies, *J. Geophys. Res.-Atmos.*, 108, 8249–8263, 2003.
- Harrison, R. M., Yin, J., Tilling, R. M., Cai, X., Seakins, P. W., Hopkins, J. R., Lansley, D. L., Lewis, A. C., Hunter, M. C., Heard, D. E., Carpenter, L. J., Creasey, D. J., Lee, J. D., Pilling, M. J., Carslaw, N., Emmerson, K. M., Redington, A., Derwent, R. G., Ryall, D., Mills, G., and Penkett, S. A.: Measurement and modelling of air pollution and atmospheric chemistry in the U.K. West Midlands conurbation: Overview of the PUMA Consortium project, *Sci. Total Environ.*, 360, 5–25, 2006.
- Heard, D. E.: Atmospheric field measurements of the hydroxyl radical using laser-induced fluorescence spectroscopy, *Annu. Rev. Phys. Chem.*, 57, 191–216, 2006.
- Heard, D. E., Carpenter, L. J., Creasey, D. J., Hopkins, J. R., Lee, J. D., Lewis, A. C., Pilling, M. J., Seakins, P. W., Carslaw, N., and Emmerson, K. M.: High levels of the hydroxyl radical in the winter urban troposphere, *Geophys. Res. Lett.*, 31, L18112–L18117, 10.1029/2004gl020544, 2004.
- Hewitt, C. N., Lee, J. D., MacKenzie, A. R., Barkley, M. P., Carslaw, N., Carver, G. D., Chappell, N. A., Coe, H., Collier, C., Commane, R., Davies, F., Davison, B., DiCarlo, P., Di Marco, C. F., Dorsey, J. R., Edwards, P. M., Evans, M. J., Fowler, D., Furneaux, K. L., Gallagher, M., Guenther, A., Heard, D. E., Helfter, C., Hopkins, J., Ingham, T., Irwin, M., Jones, C., Karunaharan, A., Langford, B., Lewis, A. C., Lim, S. F., MacDonald, S. M., Mahajan, A. S., Malpass, S., McFiggans, G., Mills, G., Misztal, P., Moller, S., Monks, P. S., Nemitz, E., Nicolas-Perea, V., Oetjen, H., Oram, D. E., Palmer, P. I., Phillips, G. J., Pike, R., Plane, J. M. C., Pugh, T., Pyle, J. A., Reeves, C. E., Robinson, N. H., Stewart, D., Stone, D., Whalley, L. K., and Yin, X.: Overview: oxidant and particle photochemical processes above a south-east Asian tropical rainforest (the OP3 project): introduction, ratio-

- nale, location characteristics and tools, *Atmos. Chem. Phys.*, 10, 169–199, doi:10.5194/acp-10-169-2010, 2010.
- Holland, F., Hofzumahaus, A., Schäfer, J., Kraus, A., and Pätz, H.-W.: Measurements of OH and HO₂ radical concentrations and photolysis frequencies during BERLIOZ, *J. Geophys. Res.-Atmos.*, 108, 8246–8261, 2003.
- Hopkins, J. R., Lewis, A. C., and Read, K. A.: A two-column method for long-term monitoring of non-methane hydrocarbons (NMHCs) and oxygenated volatile organic compounds (*o*-VOCs), *J. Environ. Monitor.*, 5, 8–13, 2003.
- Jenkin, M. E., Saunders, S. M., and Pilling, M. J.: The tropospheric degradation of volatile organic compounds: A protocol for mechanism development, *Atmos. Environ.*, 31, 81–104, 1997.
- Jenkin, M. E., Saunders, S. M., Wagner, V., and Pilling, M. J.: Protocol for the development of the Master Chemical Mechanism, MCM v3 (Part B): tropospheric degradation of aromatic volatile organic compounds, *Atmos. Chem. Phys.*, 3, 181–193, doi:10.5194/acp-3-181-2003, 2003.
- Johnson, D. and Marston, G.: The gas-phase ozonolysis of unsaturated volatile organic compounds in the troposphere, *Chem. Soc. Rev.*, 37, 699–716, 2008.
- Jones, A. R., Thomson, D. J., Hort, M., and Devenish, B.: The U.K. Met Office's next-generation atmospheric dispersion model, NAME III, in: *Air Pollution Modeling and its Application XVII (Proceedings of the 27th NATO/CCMS International Technical Meeting on Air Pollution Modelling and its Application)*, edited by: Borrego, C. and Norman, A.-L., Springer, Dordrecht, the Netherlands, 580–589, 2007.
- Kanaya, Y., Sadanaga, Y., Matsumoto, J., Sharma, U. K., Hirokawa, J., Kajii, Y., and Akimoto, H.: Nighttime observation of the HO₂ radical by an LIF instrument at Oki Island, Japan, and its possible origins, *Geophys. Res. Lett.*, 26, 2179–2182, 1999.
- Kennedy, O. J., Ouyang, B., Langridge, J. M., Daniels, M. J. S., Bauguutte, S., Freshwater, R., McLeod, M. W., Ironmonger, C., Sendall, J., Norris, O., Nightingale, R., Ball, S. M., and Jones, R. L.: An aircraft based three channel broadband cavity enhanced absorption spectrometer for simultaneous measurements of NO₃, N₂O₅ and NO₂, *Atmos. Meas. Tech.*, 4, 1759–1776, doi:10.5194/amt-4-1759-2011, 2011.
- Kroll, J. H., Clarke, J. S., Donahue, N. M., Anderson, J. G., and Demerjian, K. L.: Mechanism of HO_x Formation in the Gas-Phase Ozone-Alkene reaction. 1. Direct, Pressure-Dependent Measurements of Prompt OH Yields, *J. Phys. Chem. A*, 105, 1554–1560, 2001a.
- Kroll, J. H., Sahay, S. R., Anderson, J. G., Demerjian, K. L., and Donahue, N. M.: Mechanism of HO_x Formation in the Gas-Phase Ozone-Alkene Reaction. 2. Prompt versus Thermal Dissociation of Carbonyl Oxides to Form OH, *J. Phys. Chem. A*, 105, 4446–4457 2001b.
- Kroll, J. H., Donahue, N. M., Cee, V. J., Demerjian, K. L., and Anderson, J. G.: Gas-Phase Ozonolysis of Alkenes: Formation of OH from Anti Carbonyl Oxides, *J. Am. Chem. Soc.*, 124, 8518–8519, 2002.
- Lee, J. D., Lewis, A. C., Monks, P. S., Jacob, M., Hamilton, J. F., Hopkins, J. R., Watson, N. M., Saxton, J. E., Ennis, C., Carpenter, L. J., Carslaw, N., Fleming, Z. L., Bandy, A., Oram, D. E., Penkett, S. A., Slemr, J., Norton, E. G., Rickard, A. R., Whalley, L. K., Heard, D. E., Bloss, W. J., Gravesstock, T., Smith, S. C., Stanton, J., Pilling, M. J., and Jenkin, M. E.: Ozone photochemistry and elevated isoprene during the UK heatwave of August 2003, *Atmos. Environ.*, 40, 7598–7613, 2006.
- Lidster, R. T., Hamilton, J. F., Lee, J. D., Lewis, A. C., Hopkins, J. R., Punjabi, S., Rickard, A. R., and Young, J. C.: The impact of monoaromatic hydrocarbons on OH reactivity in the coastal UK boundary layer and free troposphere, *Atmos. Chem. Phys.*, 14, 6677–6693, doi:10.5194/acp-14-6677-2014, 2014.
- Lightfoot, P. D., Cox, R. A., Crowley, J. N., Destriau, M., Hayman, G. D., Jenkin, M. E., Moortgat, G. K., and Zabel, F.: Organic Peroxy Radicals: Kinetics, Spectroscopy and Tropospheric Chemistry, *Atmos. Environ.*, 26A, 1805–1961, 1992.
- Lou, S., Holland, F., Rohrer, F., Lu, K., Bohn, B., Brauers, T., Chang, C. C., Fuchs, H., Häseler, R., Kita, K., Kondo, Y., Li, X., Shao, M., Zeng, L., Wahner, A., Zhang, Y., Wang, W., and Hofzumahaus, A.: Atmospheric OH reactivities in the Pearl River Delta – China in summer 2006: measurement and model results, *Atmos. Chem. Phys.*, 10, 11243–11260, doi:10.5194/acp-10-11243-2010, 2010.
- Lu, K. D., Rohrer, F., Holland, F., Fuchs, H., Bohn, B., Brauers, T., Chang, C. C., Häseler, R., Hu, M., Kita, K., Kondo, Y., Li, X., Lou, S. R., Nehr, S., Shao, M., Zeng, L. M., Wahner, A., Zhang, Y. H., and Hofzumahaus, A.: Observation and modelling of OH and HO₂ concentrations in the Pearl River Delta 2006: a missing OH source in a VOC rich atmosphere, *Atmos. Chem. Phys.*, 12, 1541–1569, doi:10.5194/acp-12-1541-2012, 2012.
- Lu, K. D., Hofzumahaus, A., Holland, F., Bohn, B., Brauers, T., Fuchs, H., Hu, M., Häseler, R., Kita, K., Kondo, Y., Li, X., Lou, S. R., Oebel, A., Shao, M., Zeng, L. M., Wahner, A., Zhu, T., Zhang, Y. H., and Rohrer, F.: Missing OH source in a suburban environment near Beijing: observed and modelled OH and HO₂ concentrations in summer 2006, *Atmos. Chem. Phys.*, 13, 1057–1080, doi:10.5194/acp-13-1057-2013, 2013.
- Lu, K. D., Rohrer, F., Holland, F., Fuchs, H., Brauers, T., Oebel, A., Dlugi, R., Hu, M., Li, X., Lou, S. R., Shao, M., Zhu, T., Wahner, A., Zhang, Y. H., and Hofzumahaus, A.: Nighttime observation and chemistry of HO_x in the Pearl River Delta and Beijing in summer 2006, *Atmos. Chem. Phys.*, 14, 4979–4999, doi:10.5194/acp-14-4979-2014, 2014.
- Mauldin III, R. L., Berndt, T., Sipilä, M., Paasonen, P., Petäjä, T., Kim, S., Kurtén, A., Stratmann, F., Kerminen, V.-M., and Kulmala, M.: A new atmospherically relevant oxidant of sulphur dioxide, *Nature*, 488, 193–196, 2012.
- Morgan, W. T., Ouyang, B., Allan, J. D., Aruffo, E., Di Carlo, P., Kennedy, O. J., Lowe, D., Flynn, M. J., Rosenberg, P. D., Williams, P. I., Jones, R., McFiggans, G. B., and Coe, H.: Influence of aerosol chemical composition on N₂O₅ uptake: airborne regional measurements in northwestern Europe, *Atmos. Chem. Phys.*, 15, 973–990, doi:10.5194/acp-15-973-2015, 2015.
- Nakajima, M. and Endo, Y.: Determination of the molecular structure of the simplest Criegee intermediate CH₂OO, *J. Chem. Phys.*, 139, 101103, doi:10.1063/1.4821165, 2013.
- Nakajima, M. and Endo, Y.: Spectroscopic characterization of an alkyl substituted Criegee intermediate *syn*-CH₃CHOO through pure rotational transitions, *J. Chem. Phys.*, 140, 011101, doi:10.1063/1.4861494, 2014.
- Ouyang, B., McLeod, M. W., Jones, R. L., and Bloss, W. J.: NO₃ radical production from the reaction between the Criegee intermediate CH₂OO and NO₂, *Phys. Chem. Chem. Phys.*, 15, 17070–17075, 2013.

- Paulson, S. E., and Orlando, J. J.: The reactions of ozone with alkenes: An important source of HO_x in the boundary layer, *Geophys. Res. Lett.*, 23, 3727–3730, 1996.
- Ren, X., Harder, H., Martinez, M., Leshner, R., Olinger, A., Simpas, J. B., Brune, W. H., Schwab, J. J., Demerjian, K. L., He, Y., Zhou, X., and Gao, H.: OH and HO₂ chemistry in the urban atmosphere of New York City, *Atmos. Environ.*, 37, 3639–3651, 2003a.
- Ren, X., Harder, H., Martinez, M., Leshner, R. L., Olinger, A., Shirley, T., Adams, J., Simpas, J. B., and Brune, W. H.: HO_x concentrations and OH reactivity observations in New York City during PMTACS-NY2001, *Atmos. Environ.*, 37, 3627–3637, 2003b.
- Ren, X., Brune, W. H., Mao, J., Mitchell, M. J., Leshner, R., Simpas, J. B., Metcalf, A. R., Schwab, J. J., Cai, C., Li, Y., Demerjian, K. L., Felton, H. D., Boynton, G., Adams, A., Perry, J., He, Y., Zhou, X., and Hou, J.: Behavior of OH and HO₂ in the winter atmosphere in New York City, *Atmos. Environ.*, 40, 252–263, 2006.
- Salisbury, G., Rickard, A. R., Monks, P. S., Allan, B. J., Bauguitte, S. J. B., Penkett, S. A., Carslaw, N., Lewis, A. C., Creasey, D. J., Heard, D. E., Jacobs, P. J., and Lee, J. D.: Production of peroxy radicals at night via reactions of ozone and the nitrate radical in the marine boundary layer, *J. Geophys. Res.-Atmos.*, 106, 12669–12687, 2001.
- Saunders, S. M., Jenkin, M. E., Derwent, R. G., and Pilling, M. J.: Protocol for the development of the Master Chemical Mechanism, MCM v3 (Part A): tropospheric degradation of non-aromatic volatile organic compounds, *Atmos. Chem. Phys.*, 3, 161–180, doi:10.5194/acp-3-161-2003, 2003.
- Sheehy, P. M., Volkamer, R., Molina, L. T., and Molina, M. J.: Oxidative capacity of the Mexico City atmosphere – Part 2: A RO_x radical cycling perspective, *Atmos. Chem. Phys.*, 10, 6993–7008, doi:10.5194/acp-10-6993-2010, 2010.
- Shirley, T. R., Brune, W. H., Ren, X., Mao, J., Leshner, R., Cardenas, B., Volkamer, R., Molina, L. T., Molina, M. J., Lamb, B., Velasco, E., Jobson, T., and Alexander, M.: Atmospheric oxidation in the Mexico City Metropolitan Area (MCMA) during April 2003, *Atmos. Chem. Phys.*, 6, 2753–2765, doi:10.5194/acp-6-2753-2006, 2006.
- Smith, S. C., Lee, J. D., Bloss, W. J., Johnson, G. P., Ingham, T., and Heard, D. E.: Concentrations of OH and HO₂ radicals during NAMBLEX: measurements and steady state analysis, *Atmos. Chem. Phys.*, 6, 1435–1453, doi:10.5194/acp-6-1435-2006, 2006.
- Sommariva, R., Pilling, M. J., Bloss, W. J., Heard, D. E., Lee, J. D., Fleming, Z. L., Monks, P. S., Plane, J. M. C., Saiz-Lopez, A., Ball, S. M., Bitter, M., Jones, R. L., Brough, N., Penkett, S. A., Hopkins, J. R., Lewis, A. C., and Read, K. A.: Night-time radical chemistry during the NAMBLEX campaign, *Atmos. Chem. Phys.*, 7, 587–598, doi:10.5194/acp-7-587-2007, 2007.
- Sommariva, R., Osthoff, H. D., Brown, S. S., Bates, T. S., Baynard, T., Coffman, D., de Gouw, J. A., Goldan, P. D., Kuster, W. C., Lerner, B. M., Stark, H., Warneke, C., Williams, E. J., Fehsenfeld, F. C., Ravishankara, A. R., and Trainer, M.: Radicals in the marine boundary layer during NEAQS 2004: a model study of day-time and night-time sources and sinks, *Atmos. Chem. Phys.*, 9, 3075–3093, doi:10.5194/acp-9-3075-2009, 2009.
- Stewart, D. J., Taylor, C. M., Reeves, C. E., and McQuaid, J. B.: Biogenic nitrogen oxide emissions from soils: impact on NO_x and ozone over west Africa during AMMA (African Monsoon Multidisciplinary Analysis): observational study, *Atmos. Chem. Phys.*, 8, 2285–2297, doi:10.5194/acp-8-2285-2008, 2008.
- Still, T. J., Al-Haider, S., Seakins, P. W., Sommariva, R., Stanton, J. C., Mills, G., and Penkett, S. A.: Ambient formaldehyde measurements made at a remote marine boundary layer site during the NAMBLEX campaign – a comparison of data from chromatographic and modified Hantzsch techniques, *Atmos. Chem. Phys.*, 6, 2711–2726, doi:10.5194/acp-6-2711-2006, 2006.
- Stone, D., Evans, M. J., Commane, R., Ingham, T., Floquet, C. F. A., McQuaid, J. B., Brookes, D. M., Monks, P. S., Purvis, R., Hamilton, J. F., Hopkins, J., Lee, J., Lewis, A. C., Stewart, D., Murphy, J. G., Mills, G., Oram, D., Reeves, C. E., and Heard, D. E.: HO_x observations over West Africa during AMMA: impact of isoprene and NO_x, *Atmos. Chem. Phys.*, 10, 9415–9429, doi:10.5194/acp-10-9415-2010, 2010.
- Stone, D., Whalley, L. K., and Heard, D. E.: Tropospheric OH and HO₂ radicals: field measurements and model comparisons, *Chem. Soc. Rev.*, 41, 6348–6404, 2012.
- Stone, D., Blitz, M., Daubney, L., Howes, N. U. M., and Seakins, P.: Kinetics of CH₂OO reactions with SO₂, NO₂, NO, H₂O and CH₃CHO as a function of pressure, *Phys. Chem. Chem. Phys.*, 16, 1139–1149, 2014a.
- Stone, D., Evans, M. J., Walker, H., Ingham, T., Vaughan, S., Ouyang, B., Kennedy, O. J., McLeod, M. W., Jones, R. L., Hopkins, J., Punjabi, S., Lidster, R., Hamilton, J. F., Lee, J. D., Lewis, A. C., Carpenter, L. J., Forster, G., Oram, D. E., Reeves, C. E., Bauguitte, S., Morgan, W., Coe, H., Aruffo, E., Dari-Salisburgo, C., Giammaria, F., Di Carlo, P., and Heard, D. E.: Radical chemistry at night: comparisons between observed and modelled HO_x, NO₃ and N₂O₅ during the RONOCO project, *Atmos. Chem. Phys.*, 14, 1299–1321, doi:10.5194/acp-14-1299-2014, 2014b.
- Stutz, J., Alicke, B., Ackermann, R., Geyer, A., White, A., and Williams, E.: Vertical profiles of NO₃, N₂O₅, O₃, and NO_x in the nocturnal boundary layer: 1. Observations during the Texas Air Quality Study 2000, *J. Geophys. Res.-Atmos.*, 109, D12306–D12320, 2004.
- Su, Y.-T., Huang, Y.-H., Witek, H. A., and Lee, Y.-P.: Infrared Absorption Spectrum of the Simplest Criegee Intermediate CH₂OO, *Science*, 340, 174–176, 2013.
- Taatjes, C. A., Meloni, G., Selby, T. M., Trevitt, A. J., Osborn, D. L., Percival, C. J., and Shallcross, D. E.: Direct Observation of the Gas-Phase Criegee Intermediate (CH₂OO), *J. Am. Chem. Soc.*, 130, 11883–11885, 2008.
- Taatjes, C. A., Welz, O., Eskola, A. J., Savee, J. D., Osborn, D. L., Lee, E. P. F., Dyke, J. M., Mok, D. W. K., Shallcross, D. E., and Percival, C. J.: Direct measurement of Criegee intermediate (CH₂OO) reactions with acetone, acetaldehyde, and hexafluoroacetone, *Phys. Chem. Chem. Phys.*, 14, 10391–10400, 2012.
- Taatjes, C. A., Welz, O., Eskola, A. J., Savee, J. D., Scheer, A. M., Shallcross, D. E., Rotavera, B., Lee, E. P. F., Dyke, J. M., Mok, D. W. K., Osborn, D. L., and Percival, C. J.: Direct Measurements of Conformer-Dependent Reactivity of the Criegee Intermediate CH₃CHOO, *Science*, 340, 177–180, 2013.
- Taatjes, C. A., Shallcross, D. E., and Percival, C. J.: Research frontiers in the chemistry of Criegee intermediates and tropospheric ozonolysis, *Phys. Chem. Chem. Phys.*, 16, 1689–2180, 2014.
- Vereecken, L. and Francisco, J. S.: Theoretical studies of atmospheric reaction mechanisms in the troposphere, *Chem. Soc. Rev.*, 41, 6217–6708, 2012.

- Volkamer, R., Sheehy, P., Molina, L. T., and Molina, M. J.: Oxidative capacity of the Mexico City atmosphere – Part 1: A radical source perspective, *Atmos. Chem. Phys.*, 10, 6969–6991, doi:10.5194/acp-10-6969-2010, 2010.
- Welz, O., Savee, J. D., Osborn, D. L., Vasu, S. S., Percival, C. J., Shallcross, D. E., and Taatjes, C. A.: Direct Kinetic Measurements of Criegee Intermediate (CH₂OO) Formed by Reaction of CH₂I with O₂, *Science*, 335, 204–207, 2012.
- Whalley, L. K., Furneaux, K. L., Goddard, A., Lee, J. D., Mahajan, A., Oetjen, H., Read, K. A., Kaaden, N., Carpenter, L. J., Lewis, A. C., Plane, J. M. C., Saltzman, E. S., Wiedensohler, A., and Heard, D. E.: The chemistry of OH and HO₂ radicals in the boundary layer over the tropical Atlantic Ocean, *Atmos. Chem. Phys.*, 10, 1555–1576, doi:10.5194/acp-10-1555-2010, 2010.
- Whalley, L. K., Blitz, M. A., Desservettaz, M., Seakins, P. W., and Heard, D. E.: Reporting the sensitivity of laser-induced fluorescence instruments used for HO₂ detection to an interference from RO₂ radicals and introducing a novel approach that enables HO₂ and certain RO₂ types to be selectively measured, *Atmos. Meas. Tech.*, 6, 3425–3440, doi:10.5194/amt-6-3425-2013, 2013.
- Wong, K. W. and Stutz, J.: Influence of nocturnal vertical stability on daytime chemistry: A one-dimensional model study, *Atmos. Environ.*, 44, 3753–3760, 2010.